Hierarchical Semi-Online Optimization for Cooperative MIMO Networks with Information Parsing

Juncheng Wang, *Member, IEEE*, Min Dong, *Senior Member, IEEE*, Ben Liang, *Fellow, IEEE*, Gary Boudreau, *Senior Member, IEEE*, and Hatem Abou-Zeid, *Member, IEEE*

***Abstract*—We consider cooperative multiple-input multiple-output (MIMO) precoding design with multiple access points (APs) assisted by a central controller (CC) in a fading environment. Even though each AP may have its own local channel state information (CSI), due to the communication delay in the backhaul, neither the APs nor the CC has timely global CSI. Under this hierarchical semi-online setting, our goal is to minimize the accumulated precoding deviation, between the actual local precoders executed by the APs and an ideal cooperative precoder based on timely and perfect global CSI, subject to per-AP transmit power limits. We propose an efficient algorithm, termed Semi-Online Precoding with Information Parsing (SOPIP), which accounts for the network heterogeneity in information timeliness and computational capacity. SOPIP does not require the CC to send the full global CSI to each AP. Instead, it takes advantage of the precoder structure to substantially lower the communication overhead, while allowing each AP to effectively combine its own timely local CSI with the delayed global CSI to enable adaptive precoder updates. We analyze the performance of SOPIP in the presence of multi-slot communication delay, CSI inaccuracy, and gradient estimation error, showing that it has a bounded performance gap from an offline optimal solution. Simulation results under typical cellular system settings further demonstrate the substantial performance gain of SOPIP over other centralized and distributed schemes.**

***Index Terms*—Semi-online optimization, MIMO, cooperative precoding, CSI delay, imperfect CSI, gradient algorithm.**

I. Introduction

Multiple-input multiple-output (MIMO) and cooperative transmission have been recognized as two enabling techniques to meet the ever-increasing service demand of mobile devices [2]. In MIMO networks, each access point (AP) is equipped with multiple antennas and serves multiple mobile devices simultaneously via MIMO precoding [3]. Furthermore, cooperative transmission enables multiple APs to jointly transmit signals to the mobile devices to improve the received signal strength and mitigate interference [4]. Different cooperation schemes among APs have been proposed under various system architectures, such as coordinated multi-point transmission in cellular networks [5], cloud-radio access network [6], and cell-free massive MIMO [7]. In a cooperative wireless network, it is commonly assumed in the literature that the APs are connected to a central controller (CC) via ideal backhaul. However, in practical systems, cooperative transmission faces the challenges of non-ideal backhaul with communication delay and limited capacity.

Cooperative precoding design intrinsically requires the knowledge of global channel state information (CSI) for interference management. Therefore, most prior works adopted a *global* processing approach to design cooperative precoding at the CC, assuming the global CSI is readily available [8]-[15]. Some other works have considered distributed cooperative precoding design at the APs based only on the local CSI [16]-[18]. However, due to the lack of global CSI, such *local* processing approach cannot fully utilize the degrees of freedom available in the system to effectively mitigate interference. In contrast, the *joint* (global and local) processing approach utilizes the computational capacity at both the CC and the APs and exchanges information between them over the backhaul to achieve full degrees of freedom [19]-[23]. In this work, we adopt the joint processing approach.

All of the existing works that adopt the joint processing approach have focused on *one-shot or offline* cooperative precoding problems assuming the CSI is known beforehand. These works implicitly assume the backhaul is ideal without communication delay. However, in practical cooperative wireless networks, non-ideal backhaul can cause severe communication delay between the CC and the APs. *Online* precoding design has been considered for global processing in [24]-[26] based on delayed CSI. However, these works focused on the single-cell scenario and did not consider cooperative transmission among multiple cells. In [27], an online cooperative zero-forcing (ZF) precoding was proposed under perfect CSI. Given the practical imperfection, it is important to consider online cooperative precoding design under non-ideal backhaul in multi-cell networks. However, to the best of our knowledge, this problem has not been studied in the literature. Focusing on this problem, in this work, we consider a new *hierarchical semi-online* cooperative precoding design for joint processing, where the APs have the timely local CSI and the CC has the delayed global CSI. Besides, the delayed global CSI at the CC, we fully utilize the more recent local CSI at the APs to improve the cooperative precoding performance.

Juncheng Wang was with the University of Toronto and is now with the Department of Computer Science, Hong Kong Baptist University, Hong Kong, China (e-mail: jcwang@comp.hkbu.edu.hk).

Min Dong is with the Department of Electrical, Computer and Software Engineering, Ontario Tech University, Oshawa, ON L1G 0C5, Canada (e-mail: min.dong@ontariotechu.ca).

Ben Liang is with the Department of Electrical and Computer Engineering, University of Toronto, ON M5S 1A1, Canada (e-mail: liang@ece.utoronto.ca).

Gary Boudreau is with Ericsson Canada, Ottawa, ON K2K 2V6, Canada (e-mail: gary.boudreau@ericsson.com).

Hatem Abou-Zeid was with Ericsson Canada and is now with the Department of Electrical and Software Engineering, University of Calgary, AB T2N 1N4, Canada (e-mail: hatem.abouzeid@ucalgary.ca).

This work was supported in part by Ericsson Canada, the Natural Sciences and Engineering Research Council of Canada, and the Ontario Centre of Innovation.

A preliminary version of this work was presented in IEEE International Conference on Computer Communications (INFOCOM), 2022 [1] (DOI: 10.1109/INFOCOM48880.2022.9796813).

The challenges of hierarchical semi-online cooperative precoding design for joint processing are multi-fold. First, the design of cooperative precoding is intrinsically non-separable among the APs and therefore requires the knowledge of global CSI. Second, due to the non-ideal backhaul, neither the CC nor the APs has the timely global CSI to design the cooperative precoder. Third, besides the delayed global CSI at the CC, the APs should take full advantage of the timely local CSI to design their local precoders for improved cooperative precoding performance. Furthermore, it is important to reduce the communication overhead over the backhaul in such a hierarchical design. Besides the above challenges, in practical systems, only inaccurate CSI can be obtained at the APs. Thus, it is also critical to account for inaccurate CSI in the precoding design and analyze the impact of CSI inaccuracy on the cooperative precoding performance.

In this work, we consider cooperative MIMO precoding design with multiple APs assisted by a CC via a non-ideal backhaul with communication delay. We aim at developing a hierarchical semi-online optimization framework for a CC-assisted cooperative precoding solution that fully utilizes the timely local CSI at the APs. With only local CSI available at each AP, we formulate a cooperative precoding optimization problem to minimize the accumulated deviation between the actual local precoders executed by the APs and the idealized desired cooperative precoder. The main contributions of this paper are as follows:

- We formulate the cooperative MIMO precoding problem over non-ideal backhaul as a hierarchical semi-online optimization problem, where the APs only have timely inaccurate local CSI and require the assistance from a CC with additional computational resource and delayed inaccurate global CSI for the joint precoding design. At every time slot, each AP computes and executes its own local precoder, but all APs cooperatively minimize the accumulated deviation between the actual cooperative precoder formed by the APs and the idealized desired cooperative precoder under the perfect global CSI without delay, subject to the APs' transmit power limits. Note that due to inter-AP interference, the precoding deviation is not separable among the APs; and the communication delay between the CC and the APs may span multiple time slots.
- We propose an efficient algorithm, termed Semi-Online Precoding with Information Parsing (SOPIP), to fully account for the heterogeneity in information timeliness and computational capacity at the CC and the APs in the cooperative network. SOPIP integrates both the timely local CSI and the delayed global CSI to fully utilize the CSI timeliness for precoder updates at the CC and the APs. In particular, instead of sending the full global CSI from the CC to each AP, the algorithm efficiently parsed the channel and precoder information for the CC to send, leading to greatly reduced communication load on the backhaul. Furthermore, SOPIP performs adaptive precoder updates through multi-step gradient descent to fully utilize the available computational resources at the CC and the APs. We further develop a variant of SOPIP to accommodate multi-slot local CSI delay at the APs.
- We analyze the performance of SOPIP under the hierarchical structure, in the presence of multi-slot communication delay, CSI inaccuracy, and gradient estimation error. We show that SOPIP yields $\mathcal{O}(\max\{\tau\Pi_T, \Delta_T\})$ performance gap to the optimal solution over T time horizon using one-step gradient descent at either the CC or the APs, where τ is the total delay, Π_T (to be defined in (18)) represents the accumulated variation of the desired cooperative precoder in T slots, and Δ_T (to be defined in (20)) measures the level of variation in the gradient estimation error in T slots. We further provide an improved performance bound, which shows how the optimality gap decreases as the number of gradient descent steps increases.
- Our simulation results under typical cellular system settings show that SOPIP has fast convergence and is tolerant to a wide range of communication delay. We further demonstrate the performance advantage of SOPIP over other existing centralized and distributed schemes.

In the conference version of this work [1], we only study the problem under perfect CSI and no local CSI delay. In this extended version, we consider more general models, including inaccurate CSI and multi-slot local CSI delay, in designing SOPIP, and provide new performance analysis and simulation results under these imperfect scenarios.

Organization: The rest of this paper is organized as follows. In Section II, we present the related work. Section III describes the system model and problem formulation. In Section IV, we present SOPIP, derive its performance bounds, and discuss its performance merits. Then, in Section V, we extend SOPIP to accommodate non-zero local delay. Simulation results are presented in Section VI, followed by concluding remarks in Section VII.

Notations: The transpose, Hermitian transpose, complex conjugate, Euclidean norm, Frobenius norm, trace, and (i, j) element of a matrix $\mathbf{A}$ are denoted by $\mathbf{A}^T$, $\mathbf{A}^H$, $\mathbf{A}^*$, $\|\mathbf{A}\|$, $\|\mathbf{A}\|_F$, $\mathrm{tr}\{\mathbf{A}\}$, and $[\mathbf{A}]_{i,j}$, respectively. The notation $\mathbf{I}$ denotes an identity matrix, $\mathbb{E}_{\mathbf{a}}\{\cdot\}$ denotes the expectation over the randomness in $\mathbf{a}$, and $\Re\{\cdot\}$ denotes the real part of the enclosed parameter. For $\mathbf{g}$ being an $n \times 1$ vector, $\mathbf{g} \sim \mathcal{CN}(\mathbf{0}, \mathbf{C})$ means that $\mathbf{g}$ is a circular complex Gaussian random vector with mean $\mathbf{0}$ and covariance $\mathbf{C}$.

II. Related Work

In this section, we survey relevant existing works on cooperative precoding in offline and online scenarios.

A. One-Sided Global or Local Cooperative Precoding

Most existing works on cooperative precoding design are based on global processing at the CC (or some equivalent entity). A cooperative ZF precoding scheme was studied in [8]. In [9], the impact of synchronization on the cooperative system performance was investigated. Cooperative precoding based on the multi-cell block diagonalization technique was

proposed in [10] with per-AP transmit power limits. Compression techniques were used in [11], [12] to reduce the amount of information exchange over the backhaul. In [13], the trade-off between the backhaul cost and power consumption was investigated. Cell-free massive MIMO was proposed in [14], [15], where distributed single-antenna APs are deployed to cooperatively transmit data to the users, and the distributed APs rely on the CC for global processing. All of the above works assume the CC has the knowledge of the global CSI without delay, which is not realistic in practical cooperative networks.

Distributed cooperative precoding schemes based only on the local CSI at the APs was proposed in [16], [17]. Linear precoding was proposed in [18] for each AP based on the local CSI and the large-scale fading coefficients of the other APs. However, due to the lack of global CSI, the local processing approach may be highly suboptimal, since cooperative precoding design naturally requires the global CSI to fully utilize the degrees of freedom provided by MIMO antennas. Furthermore, they do not utilize the computation capacity of the CC to improve the system performance.

B. Joint Global and Local Cooperative Precoding

All prior works that adopt the joint global and local processing approach perform one-shot or offline optimization. Cooperative precoding design with AP clustering was considered in [19]. In [20], the local precoders were optimized through forward and backward training between the CC and APs. Cooperative transmission in a cognitive network was studied in [21]. A user mobility cooperation approach was proposed in [22] to utilize the moving users for interference mitigation. Different levels of cooperations between the CC and APs for cell-free massive MIMO systems was studied in [23]. None of these works considered the impact of backhaul communication delay on the cooperative precoding design. Furthermore, these works do not consider the channel fluctuations or provide any performance guarantees over time.

C. Online Convex Optimization for Precoding

The general online convex optimization (OCO) technique [28] accounts for the delayed information in system design. It has been applied to online precoding design problems with delayed CSI in MIMO systems. For example, online projected gradient descent was used in [24] for MIMO uplink precoding design. Dynamic precoding design for point-to-point MIMO systems was studied in [25]. Periodic precoding updates for MIMO network virtualization was considered in [26]. However, these works focused on the single-cell MIMO scenario, which cannot be applied to cooperative precoding design. Lyapunov optimization technique was applied to study online cooperative ZF precoding in multi-cell MIMO systems [27]. However, [27] focused on one-sided global precoding design based on the timely and accurate CSI, which is substantially different from this work on hierarchical precoding design with delayed and possibly inaccurate CSI.

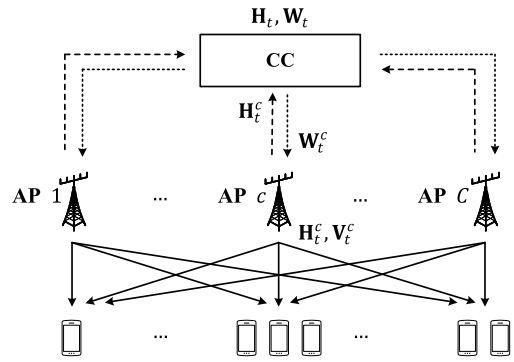

Fig. 1. An illustration of a cooperative MIMO wireless network with ideal backhaul communication links.

D. Other Related Works

A part of our proposed algorithm uses the common gradient descent method. However, different from the standard distributed online gradient descent schemes that assume separable objective functions [29]-[33], our objective function is non-separable among the APs. Therefore, distributed OCO algorithms based only on local information, such as those in [29]-[33], are not applicable to our problem. The need to consider non-ideal backhaul further adds to this challenge.

Decentralized coordinated precoding was considered in [34]-[38]. Instead of cooperatively transmitting signals to a user, the APs only focus on interference mitigation via coordination. In contrast, we focus on the scenario of cooperative transmission.

III. System Model and Problem Formulation

In this section, we will first describe a general model for cooperative MIMO networks under idealized conditions, where timely and perfect local CSI is available at each AP, and the backhaul communication experiences no delay. Following this, we will then account for CSI inaccuracy and non-ideal backhaul in our problem formulation. A further consideration for the delayed CSI at each AP will be presented in Section V. We summarize our key notations in Table I.

A. Idealized Cooperative MIMO Network Model

We consider a cooperative wireless MIMO network in a time-slotted system with time index t. As shown in Fig. 1, a total of C APs jointly serve K users with the assistance of a CC over the ideal backhaul without communication delay and error.[1] We assume each user is equipped with a single antenna. Each AP c has N^c antennas, and there are $N = \sum_{c=1}^{C} N^c$ antennas in the network. Let $\mathbf{H}_t^c \in \mathbb{C}^{K \times N^c}$ denote the local channel state between the K users and AP c at time t. Let $\mathbf{H}_t = [\mathbf{H}_t^1, \ldots, \mathbf{H}_t^C] \in \mathbb{C}^{K \times N}$ denote the global channel state between the K users and all the APs at time t. We assume the considered cooperative network is under perfect synchronization. Also, for cooperative precoding, the user messages are assumed to be available at all the APs.

[1]The AP can represent a base station, a transmission and reception point, or a remote radio unit. The CC is also referred to as central processor, central processing unit, or base-band unit pool.

TABLE I
SUMMARY OF KEY NOTATIONS

Notation	Description
T	Total number of time slots
C	Total number of APs
K	Total number of users
N	Total number of antennas
J_{CC}	Total number of gradient descent steps at CC
J_{AP}	Total number of gradient descent steps at APs
N^c	Number of antennas in AP c
u	Uplink delay from APs to CC
d	Downlink delay from CC to APs
τ_r	Round-trip delay between APs and CC
τ_l	Local delay at the APs
τ	Total delay
$\mathbf{H}_t$	Accurate global channel state at time t
$\hat{\mathbf{H}}_t$	Inaccurate global channel state at time t
$\mathbf{H}_t^c$	Accurate local channel state of AP c at time t
$\hat{\mathbf{H}}_t^c$	Inaccurate local channel state of AP c at time t
$\mathbf{V}_t$	Global cooperative precoder at time t
$\mathbf{V}_t^c$	Local precoder of AP c at time t
$\hat{\mathbf{V}}_t^{c,j}$	CC designed precoder for AP c at time t after j-step of gradient descent
$\tilde{\mathbf{V}}_t^{c,j}$	AP c designed precoder at time t after j-step of gradient descent
$\mathbf{W}_t$	Desired cooperative precoder of CC at time t
$\hat{\mathbf{W}}_t$	Inaccurate cooperative precoder of CC at time t
$\hat{\mathbf{G}}_t^c$	CC parsed global information for AP c at time t
P_{max}^c	Maximum transmit power limit at AP c
$\mathcal{V}$	Feasible set of global cooperative precoder
$\mathcal{V}^c$	Feasible set of local precoder at AP c
$\mathbf{y}_t$	Actual received signals of the K users at time t
$\tilde{\mathbf{y}}_t$	Desired received signals of the K users at time t
$\mathbf{x}_t$	Transmitted signals to the K users
$f_t(\cdot)$	Global precoding deviation at time t
$\nabla f_t^c(\cdot)$	Local gradient of AP c at time t
$\nabla \hat{f}_t^c(\cdot)$	Estimated local gradient of AP c at time t
α	Algorithm gradient descent step-size parameter
B	Channel power upper bound

At each time slot t, each AP c measures the local channel state between the K users and its N^c antennas, and observes the current local CSI $\mathbf{H}_t^c$. With possible assistance from the CC, each AP c determines its local precoder $\mathbf{V}_t^c \in \mathbb{C}^{N^c \times K}$ to the K users. Let $\mathbf{V}_t = [\mathbf{V}_t^{1\,H}, \ldots, \mathbf{V}_t^{C\,H}]^H \in \mathbb{C}^{N \times K}$ denote the cooperative precoder of all the APs, and let $\mathbf{x}_t \in \mathbb{C}^{K \times 1}$ be the signal vector intended for the K users at time slot t. We assume the signal to each user has unit power and is independent to each other, *i.e.,* $\mathbb{E}\{\mathbf{x}_t \mathbf{x}_t^H\} = \mathbf{I}, \forall t$. Each AP c has a maximum transmit power limit P_{max}^c, which leads to the following local precoder feasible set

$$\mathcal{V}^c \triangleq \{\mathbf{V}^c : \|\mathbf{V}^c\|_F^2 \leq P_{\text{max}}^c\}. \tag{1}$$

Let $\mathcal{V} \triangleq \{\mathbf{V} : \|\mathbf{V}^c\|_F^2 \leq P_{\text{max}}^c, \forall c = 1, \ldots, C\}$ be the feasible set of $\mathbf{V}_t$. The *actual* received signal vector $\mathbf{y}_t$ (noiseless) at the K users is given by

$$\mathbf{y}_t = \mathbf{H}_t \mathbf{V}_t \mathbf{x}_t. \tag{2}$$

Ideally, it is desirable for the APs to jointly design $\mathbf{V}_t$ to achieve some joint performance objective, *e.g.,* cooperative ZF precoding by all the APs to eliminate inter-user interference and maximize per-user received signal-to-noise ratio (SNR) [8]. However, such joint design would require each AP to obtain the global CSI, which is prohibitively expensive in terms of the communication overhead. Therefore, a common solution is to let a CC collect the local CSIs from APs to form the global CSI and design $\mathbf{V}_t$ centrally.

Under the perfect condition, each AP c communicates $\mathbf{H}_t^c$ to the CC without delay. With the global CSI $\mathbf{H}_t$ collected at time slot t, the CC can design a *desired* cooperative precoder $\mathbf{W}_t \in \mathbb{C}^{N \times K}$ in $\mathcal{V}$. Note that the design of $\mathbf{W}_t$ can be based on the service needs of the K users and is *not* limited to any specific precoding scheme. The desired received signal vector (noiseless) $\tilde{\mathbf{y}}_t$ is given by

$$\tilde{\mathbf{y}}_t = \mathbf{H}_t \mathbf{W}_t \mathbf{x}_t. \tag{3}$$

Again, ideally the CC communicates $\mathbf{W}_t$ to the APs without delay, and we have $\mathbf{V}_t = \mathbf{W}_t$ and $\mathbf{y}_t = \tilde{\mathbf{y}}_t$. Therefore, under the idealized case, $\mathbf{V}_t$ is not impacted by CSI delay or inaccuracy.

B. Cooperative Precoding with Delayed and Inaccurate CSI

In practical massive MIMO systems, AP c cannot obtain the accurate local CSI $\mathbf{H}_t^c$. Instead, we consider AP c only has an estimate of local CSI $\hat{\mathbf{H}}_t^c$. Furthermore, we consider non-ideal backhaul communication links between the APs and CC. Specifically, we assume the *uplink* delay in sending the local information from each AP c to the CC is u slots and the *downlink* delay for the CC to send the global information back to the APs is d slots.[2] We assume $u \geq 1$, *i.e.,* there is at least one-slot uplink delay.

Due to CSI inaccuracy and non-ideal backhaul, the actual received signal $\mathbf{y}_t$ in (2) is different from the desired $\tilde{\mathbf{y}}_t$ in (3). The expected deviation of the actual received signal vector from the desired one is given by $\mathbb{E}_{\mathbf{x}_t}\{\|\mathbf{y}_t - \tilde{\mathbf{y}}_t\|^2\} = \|\mathbf{H}_t \mathbf{V}_t - \mathbf{H}_t \mathbf{W}_t\|_F^2$. Following this, we define the precoding deviation of the APs' precoders from the CC's precoder as follows:

$$f_t(\mathbf{V}_t) \triangleq \|\mathbf{H}_t \mathbf{V}_t - \mathbf{H}_t \mathbf{W}_t\|_F^2, \quad \forall t. \tag{4}$$

Note that $f_t(\mathbf{V}_t)$ quantifies the difference between the actual local precoders and the idealized cooperative (global) precoder. We also note that, $f_t(\mathbf{V}_t)$ is strongly convex in $\mathbf{V}_t$.

The goal of our cooperative precoding design is to minimize the accumulated precoding deviation over T time slots, subject to per-AP transmit power limits. The optimization problem is formulated as follows:

$$\textbf{P1:} \quad \min_{\{\mathbf{V}_t \in \mathcal{V}\}_{t=1}^T} \quad \sum_{t=1}^T f_t(\mathbf{V}_t).$$

Note that the precoding deviation $f_t(\mathbf{V}_t)$ in (4) is *non-separable* among the APs due to the coupling of local CSI $\{\mathbf{H}_t^c\}_{c=1}^C$ and local precoders $\{\mathbf{V}_t^c\}_{c=1}^C$ creating inter-AP interference. Therefore, each AP c cannot locally solve **P1** without information exchange with other APs.

As discussed in Section I, existing works on online precoding design adopt the one-sided global processing approach, and

[2]If the APs experience different delays, the CC can synchronize the transmissions of the APs based on the maximum delay.

the designs are based solely on the delayed global CSI under the standard OCO setting. In contrast, we consider joint global and local processing in a *hierarchical* cooperative network. Furthermore, since each AP c has it own timely local CSI while the global CSI at the CC is delayed, our optimization setting is *semi-online*. Note that with delayed or inaccurate global CSI, one cannot obtain an optimal solution.[3] A widely adopted performance measure in the OCO literature [39]-[46] is the *dynamic regret* given by

$$\mathrm{RE}_T^{\mathrm{d}} \triangleq \sum_{t=1}^{T} \big(f_t(\mathbf{V}_t) - f_t(\mathbf{V}_t^{\star})\big) \tag{5}$$

where $\{\mathbf{V}_t^{\star}\}_{t=1}^T$ is an offline optimal solution assuming the accurate global CSI $\{\mathbf{H}_t\}_{t=1}^T$ is known beforehand at the CC and the backhaul communication experiences no delay. In our case, it is clear that APs set $\mathbf{V}_t^{\star} = \mathbf{W}_t$ for all t, so $\sum_{t=1}^T f_t(\mathbf{V}_t^{\star}) = 0$. Note that minimizing $\mathrm{RE}_T^{\mathrm{d}}$ is equivalent to solving **P1**.

In this paper, we consider both inaccurate CSI and non-ideal backhaul with communication delay. In this case, the APs cannot receive the ideal global precoder $\mathbf{W}_t$ from the CC in time and the actual precoder $\mathbf{V}_t$ is impacted by both CSI delay and inaccuracy. A naive solution is to directly set $\mathbf{V}_t$ as the delayed and inaccurate precoder $\hat{\mathbf{W}}_{t-u-d}$ received at the APs. However, such solution does not utilize the information timeliness of local CSI or the computational capacity at the APs. Instead, we propose a semi-online precoding design that exploits both the more timely local CSI and the available computational resource at the APs. In Section VI, we will show that our proposed solution significantly outperforms other alternatives, including the naive solution $\hat{\mathbf{W}}_{t-u-d}$ at the APs.

IV. Semi-Online Precoding with Information Parsing

In this section, we present the details of SOPIP. We combine the hierarchical semi-online setting with the gradient descent approach commonly used in the OCO literature in order to accommodate the delayed and inaccurate global CSI. However, existing online gradient descent algorithms for distributed networks, *e.g.,* [29]-[33], are not applicable to **P1**, since they implicitly assume the gradient can be computed based on the local information only. For our non-separable global objective function $f_t(\mathbf{V}_t)$ in (4), even discounting the CSI delay and inaccuracy, the *current* and *accurate* local gradient at each AP c would be given by

$$\nabla f_t^c(\mathbf{V}_t^c) \triangleq \frac{\partial f_t(\mathbf{V}_t)}{\partial \mathbf{V}_t^{c*}} = \mathbf{H}_t^{c^H}\left(\sum_{l=1}^{C}(\mathbf{H}_t^l\mathbf{V}_t^l) - \mathbf{H}_t\mathbf{W}_t\right) \tag{6}$$

where due to inter-AP interference in the received signal, $\nabla f_t^c(\mathbf{V}_t^c)$ depends on its local CSI $\mathbf{H}_t^c$, local precoder $\mathbf{V}_t^c$, and the CSI $\mathbf{H}_t^l$ and precoder $\mathbf{V}_t^l$ at any other AP $l \neq c$. Therefore, to compute its own gradient $\nabla f_t^c(\mathbf{V}_t^c)$, each AP c would need information from other APs. In SOPIP, with only local CSI available at each AP, we design joint processing algorithms at the APs and the CC to enable local gradient updates at each AP.

[3]In fact, even for the most basic centralized OCO problem with one-slot delayed and accurate information [39], an optimal solution cannot be found [40].

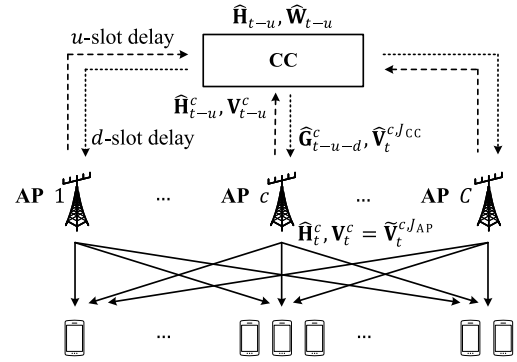

Fig. 2. An illustration of SOPIP for cooperative MIMO precoding design with delayed and inaccurate CSI.

Different from existing joint processing approaches, which do not consider the timeliness of CSI or computational capacity at the CC or the APs, our SOPIP integrates the timely local and delayed global information to enable precoder updates at both the CC and the APs. Furthermore, the number of precoder updates at both the CC and the APs can be adjustable based on the available computational resource. In the following, we describe the algorithm details of SOPIP at the CC and the APs.

A. CC's Algorithm

In practical cooperative networks, the CC often has a rich amount of computational resource that can be used for cooperative precoder design. As shown in Fig. 2, at each time slot t, each AP c determines its current local precoder $\mathbf{V}_t^c$ and then sends it together with its inaccurate local CSI $\hat{\mathbf{H}}_t^c$ to the CC. Due to the uplink delay, the CC receives the u-slot-delayed local precoder $\mathbf{V}_{t-u}^c$ and inaccurate local CSI $\hat{\mathbf{H}}_{t-u}^c$ at time slot t. The CC then then use both $\mathbf{V}_{t-u}^c$ and $\hat{\mathbf{H}}_{t-u}^c$ to update the desired cooperative precoder and generate new estimated local precoders for APs, to assist the local precoder updates at the APs.

Note that the CC needs to accommodate the downlink delay and design the precoders d slots ahead for the APs based on the u-slot-delayed information. To compute the precoder for AP c, the CC initializes an estimated precoder value $\hat{\mathbf{V}}_{t+d}^{c,0} = \mathbf{V}_{t-u}^c$ for each AP c, and performs J_{CC}-step gradient descent to generate $\hat{\mathbf{V}}_{t+d}^{c,j}, j = 1, \ldots, J_{\mathrm{CC}}$.[4] Due to the uplink delay and CSI error, the CC only has the *delayed* and *inaccurate* global CSI $\hat{\mathbf{H}}_{t-u}$ and computes the desired cooperative precoder $\hat{\mathbf{W}}_{t-u}$ that is delayed and inaccurate. Given $\hat{\mathbf{H}}_{t-u}$, $\hat{\mathbf{W}}_{t-u}$, and $\hat{\mathbf{V}}_{t+d}^{c,j-1}$, the CC generates an estimate of the local gradient at $\hat{\mathbf{V}}_{t+d}^{c,j-1}$ as

$$\nabla \hat{f}_{t-u}^c(\hat{\mathbf{V}}_{t+d}^{c,j-1}) = \hat{\mathbf{H}}_{t-u}^{c^H}\left(\sum_{l=1}^{C}(\hat{\mathbf{H}}_{t-u}^l\hat{\mathbf{V}}_{t+d}^{l,j-1}) - \hat{\mathbf{H}}_{t-u}\hat{\mathbf{W}}_{t-u}\right) \tag{7}$$

for $j = 1, \ldots, J_{\mathrm{CC}}$.

[4]Later in Sections IV-D and VI, we show that multi-step gradient descent in SOPIP improves the dynamic regret bound and the system performance.

Algorithm 1 SOPIP: CC's algorithm

Choose arbitrary $\alpha \geq B$ and broadcast it all APs.
Receive $\mathbf{V}_{t-u}^c$ and $\hat{\mathbf{H}}_{t-u}^c$ from each AP c.
Set $\hat{\mathbf{V}}_{t+d}^{c,0} = \mathbf{V}_{t-u}^c$ for each AP c.
for $j = 1$ **to** J_{CC}
  Construct estimated gradient $\nabla \hat{f}_{t-u}^c(\hat{\mathbf{V}}_{t+d}^{c,j-1})$ in (7).
  Update $\hat{\mathbf{V}}_{t+d}^{c,j}$ for each AP c via (8).
end for
Compute $\hat{\mathbf{G}}_{t-u}^c$ for each AP c via (9)
Send $\hat{\mathbf{V}}_{t+d}^{c,J_{\text{CC}}}$ and $\hat{\mathbf{G}}_{t-u}^c$ to each AP c.

Algorithm 2 SOPIP: AP c's algorithm

Initialize $\mathbf{V}_t^c \in \mathcal{V}^c$ at random for any $t \leq u$.
Receive $\hat{\mathbf{V}}_t^{c,J_{\text{CC}}}$ and $\hat{\mathbf{G}}_{t-u-d}^c$ from the CC.
Set $\tilde{\mathbf{V}}_t^{c,0} = \hat{\mathbf{V}}_t^{c,J_{\text{CC}}}$.
for $j = 1$ **to** J_{AP}
  Construct estimated gradient $\nabla \hat{f}_t^c(\tilde{\mathbf{V}}_t^{c,j-1})$ in (10).
  Update $\tilde{\mathbf{V}}_t^{c,j}$ via (11).
end for
Set $\mathbf{V}_t^c = \tilde{\mathbf{V}}_t^{c,J_{\text{AP}}}$ and execute $\mathbf{V}_t^c$.
Send $\mathbf{V}_t^c$ and $\hat{\mathbf{H}}_t^c$ to the CC.

With previous precoder update $\hat{\mathbf{V}}_{t+d}^{c,j-1}$ and gradient estimate in (7), the CC performs the following closed-form projected gradient descent to update $\hat{\mathbf{V}}_{t+d}^{c,j}$:

$$\hat{\mathbf{V}}_{t+d}^{c,j} = \mathcal{P}_{\mathcal{V}^c}\left\{\hat{\mathbf{V}}_{t+d}^{c,j-1} - \frac{1}{\alpha}\nabla \hat{f}_{t-u}^c(\hat{\mathbf{V}}_{t+d}^{c,j-1})\right\}, j = 1, \ldots, J_{\text{CC}} \quad (8)$$

where $\alpha > 0$ is a step-size parameter and $\mathcal{P}_{\mathcal{V}^c}\{\mathbf{V}^c\} \triangleq \arg\min_{\mathbf{U}^c \in \mathcal{V}^c}\{\|\mathbf{U}^c - \mathbf{V}^c\|_F^2\}$ is the projection operator onto the local convex feasible set $\mathcal{V}^c$. After the J_{CC}-step gradient descent procedure, to assist the local precoder update at each AP c, the CC then sends $\hat{\mathbf{V}}_{t+d}^{c,J_{\text{CC}}}$ to each AP c.

Furthermore, as an important feature of SOPIP, instead of sending the global CSI to every AP, the CC sends to each AP c the *parsed* global information on the precoding deviation given by

$$\hat{\mathbf{G}}_{t-u}^c = \sum_{l=1, l\neq c}^{C}\left(\hat{\mathbf{H}}_{t-u}^l \hat{\mathbf{V}}_{t+d}^{l,J_{\text{CC}}}\right) - \hat{\mathbf{H}}_{t-u}\hat{\mathbf{W}}_{t-u} \in \mathbb{C}^{K\times K}. \quad (9)$$

Compared with $\nabla \hat{f}_{t-u}^c(\hat{\mathbf{V}}_{t+d}^{c,J_{\text{CC}}})$ in (7), the global information $\hat{\mathbf{G}}_{t-u}^c$ in (9) for AP c does not contain the term $\hat{\mathbf{H}}_{t-u}^c \hat{\mathbf{V}}_{t+d}^{c,J_{\text{CC}}}$, since more timely local CSI will be used by the AP for its local precoder updates to reduce the gradient estimation error.

Note that since the global CSI is delayed and inaccurate, different from the existing global precoding design approaches, in SOPIP, the precoders generated at the CC are not used directly at the APs as the final precoders. Instead, the CC-generated estimated local precoder $\hat{\mathbf{V}}_{t+d}^{c,J_{\text{CC}}}$ along with the parsed global information $\hat{\mathbf{G}}_{t-u}^c$ are used at the APs to assist their local precoder updates.

We summarize the CC's algorithm in Algorithm 1.

B. AP's Algorithm

Recall that since the precoding deviation $f_t(\mathbf{V})$ is non-separable, each AP c cannot compute its local gradient $\nabla f_t^c(\mathbf{V}_t^c)$ in (6) based only on its local CSI. To address this issue, in SOPIP, the CC assists the local gradient estimation by communicating the parsed global information $\hat{\mathbf{G}}_{t-u}^c$ to each AP c. Note that due to the communication delay and CSI inaccuracy, the parsed global information is *delayed* and *inaccurate*.

As shown in Fig. 2, at time slot t, taking into account the additional downlink delay, each AP c receives the parsed global information $\hat{\mathbf{G}}_{t-u-d}^c$ and the estimated precoder $\hat{\mathbf{V}}_t^{c,J_{\text{CC}}}$ from the CC. Based on $\hat{\mathbf{V}}_t^{c,J_{\text{CC}}}$, each AP c initializes its own estimated local precoder $\tilde{\mathbf{V}}_t^{c,0} = \hat{\mathbf{V}}_t^{c,J_{\text{CC}}}$ and performs J_{AP}-step local gradient descent to generate $\tilde{\mathbf{V}}_t^{c,J_{\text{AP}}}$. For each gradient descent step $j = 1, \ldots, J_{\text{AP}}$, based on (6) and with the current local inaccurate CSI $\hat{\mathbf{H}}_t^c$, each AP c computes an estimate of the current local gradient at $\tilde{\mathbf{V}}_t^{c,j-1}$ as

$$\nabla \hat{f}_t^c(\tilde{\mathbf{V}}_t^{c,j-1}) = \hat{\mathbf{H}}_t^{c^H}\left(\hat{\mathbf{H}}_t^c \tilde{\mathbf{V}}_t^{c,j-1} + \hat{\mathbf{G}}_{t-u-d}^c\right). \quad (10)$$

Note that the above estimated gradient takes full advantage of the timely local CSI at the AP c, as well as the global information provided by the CC, for the local precoder updates.

Using $\tilde{\mathbf{V}}_t^{c,j-1}$ from the previous step and $\nabla \hat{f}_t^c(\tilde{\mathbf{V}}_t^{c,j-1})$ in (10), each AP c performs the following closed-form projected gradient descent to update $\tilde{\mathbf{V}}_t^{c,j}$:

$$\tilde{\mathbf{V}}_t^{c,j} = \mathcal{P}_{\mathcal{V}^c}\left\{\tilde{\mathbf{V}}_t^{c,j-1} - \frac{1}{\alpha}\nabla \hat{f}_t^c(\tilde{\mathbf{V}}_t^{c,j-1})\right\}, j = 1, \ldots, J_{\text{AP}}. \quad (11)$$

Finally, each AP c uses $\mathbf{V}_t^c = \tilde{\mathbf{V}}_t^{c,J_{\text{AP}}}$ as its local precoder for cooperative MIMO transmission with other APs at time slot t. Each AP c then communicates $\mathbf{V}_t^c$ together with the inaccurate local CSI $\hat{\mathbf{H}}_t^c$ to the CC.

We summarize AP c's algorithm in Algorithm 2.

C. Discussion on Communication and Computation

If the CC sends the exact global information $\hat{\mathbf{H}}_{t-u}$, $\hat{\mathbf{V}}_{t+d}^{J_{\text{CC}}}$, and $\hat{\mathbf{W}}_{t-u}$ to each AP c to enable its local precoder updates, the amount of communication overhead would be $3NK$. By communicating $\hat{\mathbf{V}}_{t+d}^{c,J_{\text{CC}}}$ and $\hat{\mathbf{G}}_{t-u}^c$ to each AP c, the amount of overhead is $(N^c + K)K$, which is a substantial reduction since we generally have $N \gg K$ in a massive MIMO network. Furthermore, instead of sending specific $\hat{\mathbf{G}}_{t-u}^c$ to each AP c, the CC can broadcast the shared global information $\sum_{l=1}^{C}(\hat{\mathbf{H}}_{t-u}^l \hat{\mathbf{V}}_{t+d}^{l,J_{\text{CC}}}) - \hat{\mathbf{H}}_{t-u}\hat{\mathbf{W}}_{t-u} \in \mathbb{C}^{K\times K}$ on the precoding deviation to all the APs. Each AP c can then recover $\hat{\mathbf{G}}_{t-u-d}^c$ locally by subtracting $\hat{\mathbf{H}}_{t-u-d}^c \hat{\mathbf{V}}_t^{c,J_{\text{CC}}}$ at each time slot t using its local historical CSI information $\hat{\mathbf{H}}_{t-u-d}^c$. In addition, compared with the standard single-step gradient descent algorithms, performing multi-step gradient descent at the CC (and the APs) can greatly improve the convergence speed, saving a substantial amount of overall communication overhead.

The computational complexity of the precoder updates in (8) and (11) for each AP c are dominated by matrix multiplications, which are in the order of $\mathcal{O}(NK^2)$ and $\mathcal{O}(N^cK^2)$, respectively. Note that they are similar to the complexity of

the ZF precoding scheme commonly employed for MIMO transmission in practical systems. Since only closed-form computations are involved, the overall computational complexity of SOPIP is very low at both the CC and the APs. In addition, instead of a total AP transmit power limit, per-antenna transmit power constraints at each AP c can also be incorporated into the local feasible set $\mathcal{V}^c$. In this case, we still have closed-form solutions similar to (8) and (11), with the projection operator modified to be now onto the new feasible set $\mathcal{V}^c$.

D. Performance Analysis for SOPIP

We now analyze SOPIP by providing the performance bound for it. In particular, we develop new techniques to be able to account for the multi-step gradient descent at both the CC and the APs with estimated gradients, in the presence of multi-slot delay.

We first observe that the channel power is always bounded in practice, *i.e.,* there exists some constant $B > 0$, such that

$$\|\mathbf{H}_t\|_F^2 \leq B, \quad \forall t. \tag{12}$$

In the following lemma, we show that **P1** satisfies several properties that are used in the subsequence analysis: 1) The objective function $f_t(\mathbf{V})$ is strongly convex; 2) $f_t(\mathbf{V})$ is smooth; 3) The impact of the compact convex set $\mathcal{V}$ is bounded; 4) The gradient of the objective function $\nabla f_t(\mathbf{V}) \triangleq \frac{\partial f_t(\mathbf{V})}{\partial \mathbf{V}^*}$ is bounded.

Lemma 1. Assume the bounded channel power in (12) satisfies $B \geq 2$.[5] Then, the following statements hold for any $\mathbf{U}, \mathbf{V} \in \mathcal{V}$ and any t:

$$f_t(\mathbf{U}) \geq f_t(\mathbf{V}) + \langle \nabla f_t(\mathbf{V}), \mathbf{U}-\mathbf{V}\rangle_F + \|\mathbf{U}-\mathbf{V}\|_F^2, \tag{13}$$

$$f_t(\mathbf{U}) \leq f_t(\mathbf{V}) + \langle \nabla f_t(\mathbf{V}), \mathbf{U}-\mathbf{V}\rangle_F + \frac{B}{2}\|\mathbf{U}-\mathbf{V}\|_F^2, \tag{14}$$

$$\|\mathbf{U}-\mathbf{V}\|_F \leq R, \tag{15}$$

$$\|\nabla f_t(\mathbf{V})\|_F \leq D \tag{16}$$

where $\langle \mathbf{A}, \mathbf{B}\rangle_F \triangleq 2\Re\{\mathrm{tr}\{\mathbf{A}^H\mathbf{B}\}\}$, $R = 2\sqrt{\sum_{c=1}^{C} P_{\max}^c}$, and $D = BR$.

Proof: See Appendix A.

To proceed with our analysis, we first need to quantify the impact of one-step estimated gradient descent in terms of the gradient estimation error. This is given in the following lemma. Here, for notation simplicity, we denote by $\nabla \hat{f}_t(\mathbf{V})$ a global gradient estimation function with respect to the accurate global gradient $\nabla f_t(\mathbf{V})$, which provides an upper bound on the estimation error for the local gradient estimation schemes in (7) and (10).

Lemma 2. Let $\mathbf{U} = \mathcal{P}_{\mathcal{V}}\{\mathbf{V} - \frac{1}{\alpha}\nabla \hat{f}_t(\mathbf{V})\}$. If $\alpha \geq B$ and $\gamma \in (0, 4)$, we have

$$\|\mathbf{U}-\mathbf{W}_t\|_F^2 \leq \eta\|\mathbf{V}-\mathbf{W}_t\|_F^2 + \beta\|\nabla f_t(\mathbf{V}) - \nabla \hat{f}_t(\mathbf{V})\|_F^2 \tag{17}$$

where $\eta = \frac{\alpha-2}{\alpha+2-\gamma} < 1$ and $\beta = \frac{4}{\gamma(\alpha+2-\gamma)}$.

[5]For a μ-strongly convex and L-smooth function, we always have $L \geq \mu$ [42]. For our loss function $f_t(\mathbf{V})$ in (4), we have $\mu \in (0, 2]$ and $L \in (0, B]$. To have the smallest contraction constant η in Lemma 2, we set $\mu = 2$ in (13) and therefore implicitly requires $B \geq 2$ in (14).

Proof: See Appendix B.

Remark 1. We point out a few differences of the contraction analysis in Lemma 2 and those in [42]-[44] for general OCO. From (17), the sufficient condition for $\|\mathbf{U}-\mathbf{W}_t\|_F^2 < \|\mathbf{V}-\mathbf{W}_t\|_F^2$ is $\|\nabla f_t(\mathbf{V}) - \nabla \hat{f}_t(\mathbf{V})\|_F^2 < \frac{\gamma(4-\gamma)}{4}\|\mathbf{V}-\mathbf{W}_t\|_F^2$. This condition on the gradient estimation error is most easily satisfied when $\gamma = 2$. In this case, the contraction constant $\eta = \frac{\alpha-2}{\alpha}$ recovers the one in [42]. Furthermore, as γ approaches 0, η approaches the contraction constant $\frac{\alpha-2}{\alpha+2}$ in [43]. Different from [42] and [43], our analysis takes into account the gradient estimation error and recovers the results in [42] and [43] as special cases. The contraction analysis in [44] requires additional assumptions on the gradient descent step-size and the gradient estimation error.

Next, we examine the impact of multi-step gradient descent on the dynamic regret bound of SOPIP, in the presence of both gradient estimation error and multi-slot delay. To this end, we need to quantify the accumulated variations of the underlying time-varying system. We define the accumulated variation of the globally optimal solution $\{\mathbf{W}_t\}_{T=1}^T$, which is also referred to as the path-length in the OCO literature [39], given by

$$\Pi_T \triangleq \sum_{t=1}^{T} \|\mathbf{W}_t - \mathbf{W}_{t-1}\|_F. \tag{18}$$

Another important variation measure is the squared path-length, defined as

$$\Pi_{2,T} \triangleq \sum_{t=1}^{T} \|\mathbf{W}_t - \mathbf{W}_{t-1}\|_F^2. \tag{19}$$

Note that $\Pi_{2,T}$ is often smaller than Π_T in terms of the growth order [43].[6] Further variation measures are required when we use estimated gradients. To this end, we define the accumulated gradient error as

$$\Delta_T \triangleq \sum_{t=1}^{T} \max_{\mathbf{V}\in\mathcal{V}} \|\nabla f_t(\mathbf{V}) - \nabla \hat{f}_t(\mathbf{V})\|_F, \tag{20}$$

and the accumulated squared gradient error as

$$\Delta_{2,T} \triangleq \sum_{t=1}^{T} \max_{\mathbf{V}\in\mathcal{V}} \|\nabla f_t(\mathbf{V}) - \nabla \hat{f}_t(\mathbf{V})\|_F^2. \tag{21}$$

Based on Lemmas 1-2, for any number of total gradient descent steps $J_{\text{AP}} + J_{\text{CC}} \geq 1$, we provide an upper bound on the dynamic regret RE_T^{d} of SOPIP in the following theorem. Note that the precoders designed at the CC are based on the information at time slot $t-u$ and arrive at the APs at time slot $t+d$. One can easily verify that only the round-trip delay $\tau_r = u+d$ determines the timeliness of the precoders received at the APs. Therefore, with out loss of generality, we can equivalently consider the case of τ_r-slot uplink delay and zero downlink delay in our analysis.

[6]For instance $\|\mathbf{W}_t - \mathbf{W}_{t-1}\|_F \propto T^{\kappa}$ for any t, then $\Pi_T = \mathcal{O}(T^{1+\kappa})$ and $\Pi_{2,T} = \mathcal{O}(T^{1+2\kappa})$. For a sublinear Π_T or $\Pi_{2,T}$, we have $\kappa < 0$ and therefore $\Pi_{2,T}$ is smaller than Π_T in terms of the growth rate. Particularly, if $\kappa = -\frac{1}{2}$, we have $\Pi_{2,T} = \mathcal{O}(1)$ and $\Pi_T = \mathcal{O}(T^{\frac{1}{2}})$.

Theorem 1. For $J_{\text{AP}}+J_{\text{CC}} \geq 1$, if $\alpha \geq B$, the dynamic regret yielded by SOPIP is bounded for any $\gamma \in (0,4)$ as follows:

$$\text{RE}_T^{\text{d}} \leq 2\tau_r DR + \frac{2D}{1-\sqrt{\eta^{J_{\text{AP}}+J_{\text{CC}}}}}\left(\tau_r R + \tau_r \Pi_T + \frac{2\sqrt{\beta}}{1-\sqrt{\eta}}\Delta_T\right). \tag{22}$$

Proof: We have

$$\begin{aligned}\text{RE}_T^{\text{d}} &= \sum_{t=1}^{T}\big(f_t(\mathbf{V}_t) - f_t(\mathbf{W}_t)\big)\\ &\overset{(a)}{\leq} \sum_{t=1}^{T}\langle \nabla f_t(\mathbf{V}_t), \mathbf{V}_t - \mathbf{W}_t\rangle_F\\ &\overset{(b)}{\leq} 2\sum_{t=1}^{T}\|\nabla f_t(\mathbf{V}_t)\|_F\|\mathbf{V}_t - \mathbf{W}_t\|_F\\ &\overset{(c)}{\leq} 2\tau_r DR + 2D\sum_{t=\tau_r+1}^{T}\|\mathbf{V}_t - \mathbf{W}_t\|_F \end{aligned}\tag{23}$$

where (a) follows from the convexity of $f_t(\mathbf{V})$, (b) is because $\langle \mathbf{A},\mathbf{B}\rangle_F \leq 2|\operatorname{tr}\{\mathbf{A}^H\mathbf{B}\}| \leq 2\|\mathbf{A}\|_F\|\mathbf{B}\|_F$, and (c) follows from the feasible set $\mathcal{V}$ and the gradient $\nabla f_t(\mathbf{V})$ being bounded in (15) and (16), respectively.

We now bound the RHS of (23). We have

$$\begin{aligned}&\sum_{t=\tau_r+1}^{T}\|\mathbf{V}_t - \mathbf{W}_t\|_F \overset{(a)}{\leq} \sum_{t=\tau_r+1}^{T}\Big(\sqrt{\eta^{J_{\text{AP}}}}\|\hat{\mathbf{V}}_t^{J_{\text{CC}}} - \mathbf{W}_t\|_F\\ &\quad + \sqrt{\beta}\sum_{j=1}^{J_{\text{AP}}}\sqrt{\eta}^{j-1}\|\nabla f_t(\tilde{\mathbf{V}}_t^{J_{\text{AP}}-j}) - \nabla \hat{f}_t(\tilde{\mathbf{V}}_t^{J_{\text{AP}}-j})\|_F\Big)\\ &\leq \sqrt{\eta^{J_{\text{AP}}}}\sum_{t=\tau_r+1}^{T}\|\hat{\mathbf{V}}_t^{J_{\text{CC}}} - \mathbf{W}_t\|_F\\ &\quad + \sqrt{\beta}\frac{1-\sqrt{\eta}^{J_{\text{AP}}}}{1-\sqrt{\eta}}\sum_{t=\tau_r+1}^{T}\max_{\mathbf{V}\in\mathcal{V}}\|\nabla f_t(\mathbf{V}) - \nabla \hat{f}_t(\mathbf{V})\|_F\\ &\overset{(b)}{\leq} \sqrt{\eta^{J_{\text{AP}}}}\sum_{t=\tau_r+1}^{T}\|\hat{\mathbf{V}}_t^{J_{\text{CC}}} - \mathbf{W}_t\|_F + \frac{\sqrt{\beta}\Delta_T}{1-\sqrt{\eta}}\end{aligned}\tag{24}$$

where (a) follows from applying Lemma 2 to (11) for J_{AP} times and $\|\mathbf{A}\|_F^2 + \|\mathbf{B}\|_F^2 \leq (\|\mathbf{A}\|_F + \|\mathbf{B}\|_F)^2$ such that $\|\tilde{\mathbf{V}}_t^j - \mathbf{W}_t\|_F \leq \sqrt{\eta}\|\tilde{\mathbf{V}}_t^{j-1} - \mathbf{W}_t\|_F + \sqrt{\beta}\|\nabla f_t(\tilde{\mathbf{V}}_t^{j-1}) - \nabla \hat{f}_t(\tilde{\mathbf{V}}_t^{j-1})\|_F, \forall j = 1,\ldots,J_{\text{AP}}$, and (b) is because of the definition of Δ_T in (18) and $\eta < 1$.

We continue to bound the first term on the RHS of (24) as follows:

$$\begin{aligned}&\sum_{t=\tau_r+1}^{T}\|\hat{\mathbf{V}}_t^{J_{\text{CC}}} - \mathbf{W}_t\|_F\\ &\overset{(a)}{\leq} \sum_{t=\tau_r+1}^{T}\Big(\|\hat{\mathbf{V}}_t^{J_{\text{CC}}} - \mathbf{W}_{t-\tau_r}\|_F + \|\mathbf{W}_t - \mathbf{W}_{t-\tau_r}\|_F\Big)\\ &\overset{(b)}{\leq} \sqrt{\eta^{J_{\text{CC}}}}\sum_{t=\tau_r+1}^{T}\|\mathbf{V}_{t-\tau_r} - \mathbf{W}_{t-\tau_r}\|_F + \frac{\sqrt{\beta}\Delta_T}{1-\sqrt{\eta}} + \tau_r\Pi_T\end{aligned}\tag{25}$$

where (a) is because $\|\mathbf{A}+\mathbf{B}\|_F \leq \|\mathbf{A}\|_F + \|\mathbf{B}\|_F$ and (b) follows from applying Lemma 2 to (8) for J_{CC} times similar to the proof of (24) and the definition of Π_T.

Substituting (25) into (24), and rearranging terms, we have

$$\begin{aligned}&\Big(1-\sqrt{\eta^{J_{\text{AP}}+J_{\text{CC}}}}\Big)\sum_{t=\tau_r+1}^{T}\|\mathbf{V}_t - \mathbf{W}_t\|_F - \sqrt{\eta^{J_{\text{AP}}+J_{\text{CC}}}}\sum_{t=1}^{\tau_r}\|\mathbf{V}_t - \mathbf{W}_t\|_F\\ &\leq \sqrt{\eta^{J_{\text{AP}}}}\tau_r\Pi_T + \frac{(\sqrt{\eta^{J_{\text{AP}}}}+1)\sqrt{\beta}}{1-\eta}\Delta_T.\end{aligned}\tag{26}$$

Substituting (26) into (23) and noting that $\eta < 1$ and the feasible set $\mathcal{V}$ being bounded in (15), we have (22). ■

The dynamic regret bound (22) in Theorem 1 improves as the total number of gradient descent steps $J_{\text{AP}}+J_{\text{CC}}$ increases. When $J_{\text{AP}} + J_{\text{CC}}$ is sufficiently large, we provide another dynamic regret bound for SOPIP below.

Theorem 2. For $J_{\text{AP}}+J_{\text{CC}} > \log_\eta(\frac{1}{2})$, if $\alpha \geq B$, the dynamic regret yielded by SOPIP is bounded for any $\gamma \in (0,4)$ as follows:

$$\text{RE}_T^{\text{d}} \leq \frac{B}{2(1-2\eta^{J_{\text{AP}}+J_{\text{CC}}})}\left(2\tau_r R^2 + 2\tau_r^2\Pi_{2,T} + \frac{3\beta}{1-\eta}\Delta_{2,T}\right). \tag{27}$$

Proof: We have

$$\begin{aligned}\text{RE}_T^{\text{d}} &\overset{(a)}{\leq} \sum_{t=1}^{T}\langle \nabla f_t(\mathbf{W}_t), \mathbf{V}_t - \mathbf{W}_t\rangle_F + \frac{B}{2}\|\mathbf{V}_t - \mathbf{W}_t\|_F^2\\ &\overset{(b)}{\leq} \frac{B}{2}\tau_r R^2 + \frac{B}{2}\sum_{t=\tau_r+1}^{T}\|\mathbf{V}_t - \mathbf{W}_t\|_F^2\end{aligned}\tag{28}$$

where (a) follows from the objective function $f_t(\mathbf{V})$ being B-smooth in (14), and (b) is because $\nabla f_t(\mathbf{W}_t) = \mathbf{0}$ and the feasible set $\mathcal{V}$ being bounded in (15).

We now bound the RHS of (28). We have

$$\begin{aligned}&\sum_{t=\tau_r+1}^{T}\|\mathbf{V}_t - \mathbf{W}_t\|_F^2 \overset{(a)}{\leq} \sum_{t=\tau_r+1}^{T}\Big(\eta^{J_{\text{AP}}}\|\hat{\mathbf{V}}_t^{J_{\text{CC}}} - \mathbf{W}_t\|_F^2\\ &\quad + \beta\sum_{j=1}^{J_{\text{AP}}}\eta^{j-1}\|\nabla \hat{f}_t(\tilde{\mathbf{V}}_t^{J_{\text{AP}}-j}) - \nabla f_t(\tilde{\mathbf{V}}_t^{J_{\text{AP}}-j})\|_F^2\Big)\\ &\leq \eta^{J_{\text{AP}}}\sum_{t=\tau_r+1}^{T}\|\hat{\mathbf{V}}_t^{J_{\text{CC}}} - \mathbf{W}_t\|_F^2\\ &\quad + \beta\frac{1-\eta^{J_{\text{AP}}}}{1-\eta}\sum_{t=\tau_r+1}^{T}\max_{\mathbf{V}\in\mathcal{V}}\|\nabla \hat{f}_t(\mathbf{V}) - \nabla f_t(\mathbf{V})\|_F^2\\ &\overset{(b)}{\leq} \eta^{J_{\text{AP}}}\sum_{t=\tau_r+1}^{T}\|\hat{\mathbf{V}}_t^{J_{\text{CC}}} - \mathbf{W}_t\|_F + \frac{\beta\Delta_{2,T}}{1-\eta}\end{aligned}\tag{29}$$

where (a) follows from applying Lemma 2 to (11) for J_{AP} times and (b) is because $\Delta_{2,T}$ being defined in (21) and $\eta < 1$.

We continue to bound the RHS of (29) as follows:

$$\begin{aligned}&\sum_{t=\tau_r+1}^{T}\|\hat{\mathbf{V}}_t^{J_{\text{CC}}} - \mathbf{W}_t\|_F^2\\ &\overset{(a)}{\leq} 2\sum_{t=\tau_r+1}^{T}\big(\|\hat{\mathbf{V}}_t^{J_{\text{CC}}} - \mathbf{W}_{t-\tau_r}\|_F^2 + \|\mathbf{W}_t - \mathbf{W}_{t-\tau_r}\|_F^2\big)\end{aligned}$$

$$\overset{(b)}{\leq} 2\sum_{t=\tau_r+1}^{T}\|\hat{\mathbf{V}}_t^{J_{\text{CC}}}-\mathbf{W}_{t-\tau_r}\|_F^2+2\tau_r^2\Pi_{2,T}$$
$$\overset{(c)}{\leq} 2\eta^{J_{\text{CC}}}\sum_{t=\tau_r+1}^{T}\|\mathbf{V}_{t-\tau_r}-\mathbf{W}_{t-\tau_r}\|_F^2+\frac{2\beta\Delta_{2,T}}{1-\eta}+2\tau_r^2\Pi_{2,T} \tag{30}$$

where (a) is because $\|\mathbf{A}+\mathbf{B}\|_F^2 \leq 2(\|\mathbf{A}\|_F^2+\|\mathbf{B}\|_F^2)$, (b) follows from $\|\mathbf{W}_t-\mathbf{W}_{t-\tau_r}\|_F^2 \leq \tau_r\sum_{i=1}^{\tau_r}\|\mathbf{W}_{t-\tau_r+i}-\mathbf{W}_{t-\tau_r+i-1}\|_F^2$ and the definition of $\Pi_{2,T}$ in (19), and (c) follows from applying Lemma 2 to (8) for J_{CC} times similar to (29).

Substituting (30) into (29) and rearranging terms, we have

$$\big(1-2\eta^{J_{\text{AP}}+J_{\text{CC}}}\big)\sum_{t=\tau_r+1}^{T}\|\mathbf{V}_t-\mathbf{W}_t\|_F^2-2\eta^{J_{\text{AP}}+J_{\text{CC}}}\sum_{t=1}^{\tau_r}\|\mathbf{V}_t-\mathbf{W}_t\|_F^2$$
$$\leq 2\eta^{J_{\text{AP}}}\tau_r^2\Pi_{2,T}+\frac{(2\eta^{J_{\text{AP}}}+1)\beta}{1-\eta}\Delta_{2,T}. \tag{31}$$

Substituting (31) into (28), noting that $\eta < 1$ and the radius of $\mathcal{V}$ being bounded in (15), and on the condition that $2\eta^{J_{\text{AP}}+J_{\text{CC}}} < 1$, we have (27). ■

From Theorems 1 and 2, we directly conclude the growth rates of the dynamic regret of SOPIP in the following corollary. The proof can be obtained by removing the constant terms in (22) and (27) under the total number of gradient descent steps $J_{\text{AP}}+J_{\text{CC}}$ specified in Theorems 1 and 2, respectively, and is omitted for brevity.

Corollary 1. For $J_{\text{AP}}+J_{\text{CC}} \geq 1$, we have

$$\text{RE}_T^{\text{d}} = \mathcal{O}(\max\{\tau_r\Pi_T, \Delta_T\}). \tag{32}$$

For $J_{\text{AP}}+J_{\text{CC}} > \log_\eta(\frac{1}{2})$, we have

$$\text{RE}_T^{\text{d}} = \mathcal{O}\big(\min\big\{\max\{\tau_r\Pi_T, \Delta_T\}, \max\{\tau_r^2\Pi_{2,T}, \Delta_{2,T}\}\big\}\big). \tag{33}$$

Remark 2. Note that the feedback delay is always bounded by some constant in practice, *i.e.,* $\tau_r = \mathcal{O}(1)$. Thus, from Corollary 1, a sufficient condition for SOPIP to yield sublinear dynamic regret is either $\max\{\Pi_T, \Delta_T\} = o(T)$ or $\max\{\Pi_{2,T}, \Delta_{2,T}\} = o(T)$, *i.e.,* the variation measures grow sublinearly over time. The significance of achieving sublinear dynamic regret is that it implies the time-averaged precoding deviation converges to zero as T goes to infinity. Furthermore, note that sublinearity of the variation measures is necessary to have sublinear dynamic regret for a system with delayed system information. This can be seen from the dynamic regret bounds derived in the OCO literature [39]-[46]. In systems that stabilize over time, leading to sublinear variation measures, we have sublinear dynamic regret.

Remark 3. To further understand the differences between SOPIP and the existing general OCO algorithms, note that the semi-online joint global and local gradient descent structure of SOPIP may be viewed as a generalization of several existing studies on generic OCO with strongly convex and smooth objective functions [42]-[44]. However, all of these works consider only centralized gradient descent, and they are limited to one-slot information delay. With one-step and multi-step gradient descent algorithms, $\mathcal{O}(\Pi_T)$ and $\mathcal{O}(\min\{\Pi_T, \Pi_{2,T}\})$ dynamic regrets were achieved in [42] and [43], respectively, while [44] showed that $\mathcal{O}(\max\{\Pi_T, \Delta_T\})$ dynamic regret can be achieved with one-step gradient descent using inexact gradients. It is easy to see that these regret bounds are special cases of the ones yielded by SOPIP in (32) and (33).

V. SOPIP with Local CSI Delay

In the previous section, we have proposed SOPIP assuming the local CSI at each AP experiences no delay. In practice, there often is delay in obtaining the CSI. This is the case especially for MIMO fading channels, where the channel varies over time and the feedback resource is limited. Thus, in this section, we extend SOPIP to the case of delayed local CSI at the APs. Note that local CSI delay affects transmission at both the APs and the CC, since precoder updates and information parsing happen at both the APs and the CC in the considered hierarchical cooperative network. Therefore, inaccurate CSI and delay due to non-ideal backhaul further complicate the consideration of local CSI delay in SOPIP. We will further study the impact of the delayed local CSI on system performance.

We now consider the scenario where the APs receive their local CSI after $\tau_l > 0$ time slots. Specifically, each AP c only has the τ_l-delayed inaccurate local CSI $\hat{\mathbf{H}}_{t-\tau_l}^c$ at each time slot t. Let $\tau = \tau_l + \tau_r$ be the total delay. Below, We extend Algorithms 1 and 2 to handle τ_l-delayed local CSI, where the modifications are mainly on the time stamps of the gradient estimation, precoder update, and information parsing in (7)-(11).[7] SOPIP with local delay for CC and AP c are summarized in Algorithm 3 and 4, respectively.

To extend Algorithm 1 to Algorithm 3, we make the following modifications: i) Start the algorithm at $t > \tau$; ii) In Step 2, change $\mathbf{V}_{t-u}^c$ and $\hat{\mathbf{H}}_{t-u}^c$ to $\mathbf{V}_{t-\tau}^c$ and $\hat{\mathbf{H}}_{t-\tau}^c$, respectively; iii) In Step 3, set $\hat{\mathbf{V}}_t^{c,0} = \mathbf{V}_{t-\tau}^c$; iv) In Step 5, construct gradient $\nabla\hat{f}_{t-\tau}^c(\hat{\mathbf{V}}_t^{c,j-1})$ in (7) with $\hat{\mathbf{H}}_{t-u}$ and $\hat{\mathbf{W}}_{t-u}$ replaced by $\hat{\mathbf{H}}_{t-\tau}$ and $\hat{\mathbf{W}}_{t-\tau}$, respectively; v) In Step 6, update precoder $\hat{\mathbf{V}}_t^{c,j}$ using $\nabla\hat{f}_{t-\tau}^c(\hat{\mathbf{V}}_t^{c,j-1})$ instead of $\nabla\hat{f}_{t-u}^c(\hat{\mathbf{V}}_{t+d}^{c,j-1})$; vi) In Step 8, construct global information $\hat{\mathbf{G}}_{t-\tau}^c$ in (9) with $\hat{\mathbf{H}}_{t-u}$ and $\hat{\mathbf{W}}_{t-u}$ replaced by $\hat{\mathbf{H}}_{t-\tau}$ and $\hat{\mathbf{W}}_{t-\tau}$, respectively; vii) In Step 9, modify $\hat{\mathbf{V}}_{t+d}^{c,J_{\text{CC}}}$ and $\hat{\mathbf{G}}_{t-u}$ to $\hat{\mathbf{V}}_t^{c,J_{\text{CC}}}$ and $\hat{\mathbf{G}}_{t-\tau}$, respectively.

We make the following changes to extend Algorithm 2 to Algorithm 4: i) Start the algorithm at $t > \tau$; ii) In Step 3, change $\hat{\mathbf{G}}_{t-u-d}^c$ to $\hat{\mathbf{G}}_{t-\tau}^c$; iii) In Step 5, construct gradient $\nabla\hat{f}_{t-\tau_l}^c(\tilde{\mathbf{V}}_t^{c,j-1})$ in (10) with $\hat{\mathbf{H}}_t^c$ and $\hat{\mathbf{G}}_{t-u-d}^c$ replaced by $\hat{\mathbf{H}}_{t-\tau_l}^c$ and $\hat{\mathbf{G}}_{t-\tau}^c$, respectively; iv) In Step 6, update precoder $\tilde{\mathbf{V}}_t^{c,j}$ using $\nabla\hat{f}_{t-\tau_l}^c(\tilde{\mathbf{V}}_t^{c,j-1})$ instead of $\nabla\hat{f}_t^c(\tilde{\mathbf{V}}_t^{c,j-1})$; v) In Step 9, modify $\hat{\mathbf{H}}_t^c$ to $\hat{\mathbf{H}}_{t-\tau_l}^c$.

Using similar techniques as those in the proofs of Theorem 1 and 2, we provide dynamic regret bounds for SOPIP with local delay under different values of the total gradient descent steps $J_{\text{AP}}+J_{\text{CC}}$ in the following theorem.

[7] A more recent precoder $\mathbf{V}_{t-\tau_l}^c$ than the less recent CSI $\hat{\mathbf{H}}_{t-\tau}^c$ at the CC does not help improve the accuracy of gradient estimation. Therefore, the timeliness of $\mathbf{V}_{t-\tau_l}^c$ is not useful at the CC.

Algorithm 3 SOPIP with local CSI delay: CC's algorithm

Choose arbitrary $\alpha \geq B$ and broadcast it all APs.
Receive $\mathbf{V}_{t-\tau}^c$ and $\hat{\mathbf{H}}_{t-\tau}^c$ from each AP c.
Set $\hat{\mathbf{V}}_t^{c,0} = \mathbf{V}_{t-\tau}^c$ for each AP c.
for $j = 1$ **to** J_{CC}
  Construct estimated gradient $\nabla \hat{f}_{t-\tau}^c(\hat{\mathbf{V}}_t^{c,j-1})$ via

$$\nabla \hat{f}_{t-\tau}^c(\hat{\mathbf{V}}_t^{c,j-1}) = \hat{\mathbf{H}}_{t-\tau}^{c^H}\Big(\sum_{l=1}^{C}(\hat{\mathbf{H}}_{t-\tau}^l \hat{\mathbf{V}}_t^{l,j-1}) - \hat{\mathbf{H}}_{t-\tau}\hat{\mathbf{W}}_{t-\tau}\Big).$$

  Update $\hat{\mathbf{V}}_t^{c,j}$ for each AP c via

$$\hat{\mathbf{V}}_t^{c,j} = \mathcal{P}_{\mathcal{V}^c}\left\{\hat{\mathbf{V}}_t^{c,j-1} - \frac{1}{\alpha}\nabla \hat{f}_{t-\tau}^c(\hat{\mathbf{V}}_t^{c,j-1})\right\}. \quad (34)$$

end for
Compute $\hat{\mathbf{G}}_{t-\tau}^c$ for each AP c via

$$\hat{\mathbf{G}}_{t-\tau}^c = \left(\hat{\mathbf{H}}_{t-\tau}^l \hat{\mathbf{V}}_t^{l,J_{\text{CC}}}\right) - \hat{\mathbf{H}}_{t-\tau}\hat{\mathbf{W}}_{t-\tau}$$

Send $\hat{\mathbf{V}}_t^{c,J_{\text{CC}}}$ and $\hat{\mathbf{G}}_{t-\tau}^c$ to each AP c.

Theorem 3. If $\alpha \geq B$, the dynamic regret yielded by SOPIP with local delay is bounded for any $\gamma \in (0, 4)$ as follows:

i) For $J_{\text{AP}} + J_{\text{CC}} \geq 1$, we have

$$\text{RE}_T^{\text{d}} \leq 2\tau DR + \frac{D}{1-\sqrt{\eta^{J_{\text{AP}}+J_{\text{CC}}}}}\Big(\tau R + \tau\Pi_T + \frac{2\sqrt{\beta}}{1-\sqrt{\eta}}\Delta_T\Big). \quad (35)$$

ii) For $J_{\text{AP}} + J_{\text{CC}} > \log_\eta(\frac{1}{4})$, we have

$$\text{RE}_T^{\text{d}} \leq \frac{B}{2(1-4\eta^{J_{\text{AP}}+J_{\text{CC}}})}\Big(5\tau R^2 + (2\tau_l^2 + 4\tau_r^2)\Pi_{2,T} + \frac{6\beta}{1-\eta}\Delta_{2,T}\Big). \quad (36)$$

Proof: We first prove (35). We can show that (23) still holds by replacing τ_r with τ. Similar to the proof of (24) and (25), applying Lemma 2 to (38) and (34) for J_{AP} and J_{CC} times, respectively, we can show that

$$\begin{aligned}
&\sum_{t=\tau+1}^{T}\|\mathbf{V}_t - \mathbf{W}_t\|_F \leq \tau_l\Pi_T + \sum_{t=\tau+1}^{T}\|\mathbf{V}_t - \mathbf{W}_{t-\tau_l}\|_F \\
&\leq \tau_l\Pi_T + \sqrt{\eta^{J_{\text{AP}}}}\sum_{t=\tau+1}^{T}\|\hat{\mathbf{V}}_t^{J_{\text{CC}}} - \mathbf{W}_{t-\tau_l}\|_F + \frac{\sqrt{\beta}\Delta_T}{1-\sqrt{\eta}} \\
&\leq \tau_l\Pi_T + \sqrt{\eta^{J_{\text{AP}}}}\tau_r\Pi_T + \sqrt{\eta^{J_{\text{AP}}+J_{\text{CC}}}}\sum_{t=\tau+1}^{T}\|\mathbf{V}_{t-\tau} - \mathbf{W}_{t-\tau}\|_F \\
&\quad + \frac{(\sqrt{\eta^{J_{\text{AP}}}}+1)\sqrt{\beta}\Delta_T}{1-\sqrt{\eta}}. \quad (37)
\end{aligned}$$

Substituting (37) into the version of (23) with τ_r replaced by τ and following the proof of (26), we have (35).

We now prove (36). We have

$$\begin{aligned}
&\sum_{t=\tau+1}^{T}\|\mathbf{V}_t - \mathbf{W}_t\|_F^2 \\
&\leq 2\sum_{t=\tau+1}^{T}\left(\|\mathbf{V}_t - \mathbf{W}_{t-\tau_l}\|_F^2 + \|\mathbf{W}_t - \mathbf{W}_{t-\tau_l}\|_F^2\right) \\
&\leq 2\tau_l^2\Pi_{2,T} + 2\sum_{t=\tau+1}^{T}\|\mathbf{V}_t - \mathbf{W}_{t-\tau_l}\|_F^2. \quad (39)
\end{aligned}$$

Algorithm 4 SOPIP with local CSI delay: AP c's algorithm

Initialize $\mathbf{V}_t^c \in \mathcal{V}^c$ at random for any $t \leq \tau$.
Receive $\hat{\mathbf{V}}_t^{c,J_{\text{CC}}}$ and $\hat{\mathbf{G}}_{t-\tau}^c$ from the CC.
Set $\tilde{\mathbf{V}}_t^{c,0} = \hat{\mathbf{V}}_t^{c,J_{\text{CC}}}$.
for $j = 1$ **to** J_{AP}
  Construct estimated gradient $\nabla \hat{f}_{t-\tau_l}^c(\tilde{\mathbf{V}}_t^{c,j-1})$ via

$$\nabla \hat{f}_{t-\tau_l}^c(\tilde{\mathbf{V}}_t^{c,j-1}) = \hat{\mathbf{H}}_{t-\tau_l}^{c^H}\left(\hat{\mathbf{H}}_{t-\tau_l}^c \hat{\mathbf{V}}_t^{c,j-1} + \hat{\mathbf{G}}_{t-\tau}^c\right).$$

  Update $\tilde{\mathbf{V}}_t^{c,j}$ via (11).

$$\tilde{\mathbf{V}}_t^{c,j} = \mathcal{P}_{\mathcal{V}^c}\left\{\tilde{\mathbf{V}}_t^{c,j-1} - \frac{1}{\alpha}\nabla \hat{f}_{t-\tau_l}^c(\tilde{\mathbf{V}}_t^{c,j-1})\right\}. \quad (38)$$

end for
Set $\mathbf{V}_t^c = \tilde{\mathbf{V}}_t^{c,J_{\text{AP}}}$ and execute $\mathbf{V}_t^c$.
Send $\mathbf{V}_t^c$ and $\hat{\mathbf{H}}_{t-\tau_l}^c$ to the CC.

Similar to the proof of (29) and (30), applying Lemma 2 to (38) and (34) for J_{AP} and J_{CC} times, respectively, we can show that

$$\begin{aligned}
&\sum_{t=\tau+1}^{T}\|\mathbf{V}_t - \mathbf{W}_{t-\tau_l}\|_F^2 \\
&\leq \eta^{J_{\text{AP}}}\sum_{t=\tau+1}^{T}\|\hat{\mathbf{V}}_t^{J_{\text{CC}}} - \mathbf{W}_{t-\tau_l}\|_F^2 + \frac{\beta\Delta_{2,T}}{1-\eta} \\
&\leq 2\eta^{J_{\text{AP}}}\sum_{t=\tau+1}^{T}\|\hat{\mathbf{V}}_t^{J_{\text{CC}}} - \mathbf{W}_{t-\tau}\|_F^2 + 2\eta^{J_{\text{AP}}}\tau_r^2\Pi_{2,T} + \frac{\beta\Delta_{2,T}}{1-\eta} \\
&\leq 2\eta^{J_{\text{AP}}+J_{\text{CC}}}\sum_{t=\tau+1}^{T}\|\mathbf{V}_{t-\tau} - \mathbf{W}_{t-\tau}\|_F^2 + 2\eta^{J_{\text{AP}}}\tau_r^2\Pi_{2,T} \\
&\quad + \frac{(2\eta^{J_{\text{AP}}}+1)\beta\Delta_{2,T}}{1-\eta}. \quad (40)
\end{aligned}$$

Substituting (40) into (39) and rearranging terms, we have

$$\begin{aligned}
&(1-4\eta^{J_{\text{AP}}+J_{\text{CC}}})\sum_{t=\tau+1}^{T}\|\mathbf{V}_t - \mathbf{W}_t\|_F^2 - 4\eta^{J_{\text{AP}}+J_{\text{CC}}}\sum_{t=1}^{\tau}\|\mathbf{V}_t - \mathbf{W}_t\|_F^2 \\
&\leq (2\tau_l^2 + 4\eta^{J_{\text{AP}}}\tau_r^2)\Pi_{2,T} + \frac{(4\eta^{J_{\text{AP}}}+2)\beta\Delta_{2,T}}{1-\eta}. \quad (41)
\end{aligned}$$

We can show that (28) still holds by replacing τ_r with τ. Substituting (41) into the version of (28) with τ_r replaced by τ, and noting that $\eta < 1$ and $4\eta^{J_{\text{AP}}+J_{\text{CC}}} < 1$, we have (36). ■

From Theorem 3, we can derive the growth rates of the dynamic regret of SOPIP under different total numbers of gradient descent steps $J_{\text{CC}} + J_{\text{AP}}$ in the following corollary. The proof follows directly from removing the constant terms in (35) and (36) under the total number of gradient descent steps $J_{\text{CC}} + J_{\text{AP}}$ specified in Theorem 3, respectively, and is omitted for brevity.

Corollary 2. For $J_{\text{AP}} + J_{\text{CC}} \geq 1$, we have

$$\text{RE}_T^{\text{d}} = \mathcal{O}(\max\{\tau\Pi_T, \Delta_T\}). \quad (42)$$

TABLE II
DYNAMIC REGRET OF SOPIP

$\tau_l > 0$	$J_{\text{CC}} + J_{\text{AP}}$	RE_T^{d}
No	≥ 1	$\mathcal{O}(\max\{\tau_r \Pi_T, \Delta_T\})$
No	$> \log_\eta(\frac{1}{2})$	$\mathcal{O}\left(\min\left\{\max\{\tau_r \Pi_T, \Delta_T\}, \max\{\tau_r^2 \Pi_{2,T}, \Delta_{2,T}\}\right\}\right)$
Yes	≥ 1	$\mathcal{O}(\max\{\tau \Pi_T, \Delta_T\})$
Yes	$> \log_\eta(\frac{1}{4})$	$\mathcal{O}\left(\min\left\{\max\{\tau \Pi_T, \Delta_T\}, \max\{\tau^2 \Pi_{2,T}, \Delta_{2,T}\}\right\}\right)$

For $J_{\text{AP}} + J_{\text{CC}} > \log_\eta(\frac{1}{4})$, we have

$$\text{RE}_T^{\text{d}} = \mathcal{O}\big(\min\big\{\max\{\tau \Pi_T, \Delta_T\}, \max\{\tau^2 \Pi_{2,T}, \Delta_{2,T}\}\big\}\big). \quad (43)$$

From Corollary 2, the total number of gradient descent steps $J_{\text{AP}} + J_{\text{CC}}$ needs to be larger than $\log_\eta(\frac{1}{4})$ for (43). This condition is more stringent than the condition $J_{\text{AP}} + J_{\text{CC}} > \log_\eta(\frac{1}{2})$ in Corollary 1 for (33) due to the additional local delay. However, the growth rates of the dynamic regret bounds in Corollary 2 are still dominated by the accumulated system variation measures Π_T, $\Pi_{2,T}$, Δ_T, and $\Delta_{2,T}$, and are the same as those in Corollary 1 without local delay. We summarize the dynamic regret of SOPIP under different conditions in Table II.

VI. Simulation Results

In this section, under typical cellular system settings, we study the impacts of various system parameters on the convergence and performance of SOPIP and demonstrate the performance advantage of SOPIP over other centralized and distributed alternatives.[8]

A. Simulation Setup

We consider an urban micro-cell of radius 500 m, with $C = 3$ APs equally spaced to each other with 250 m distance to the cell center. Each AP c is equipped with $N^c = 16$ antennas by default. We set 5 co-located users at the mid-point between every two adjacent APs, for a total of $K = 15$ users in the network by default. Different N and K values will be studied later.

Following the typical cellular system settings [47], we consider transmission over one subcarrier of bandwidth $B_W = 15$ kHz and set one time slot to one symbol duration $\frac{1}{B_W} = 66.7$ μs. We set the maximum transmit power limit $P_{\max}^c = 30$ dBm for all c. The receiver thermal noise power spectral density is $N_0 = -174$ dBm/Hz and noise figure is $N_F = 10$ dB. We model the fading channel between AP c and user k over time as a first-order Gauss-Markov process [48] given by $\mathbf{h}_{t+1}^{c,k} = \alpha_{\mathbf{h}} \mathbf{h}_t^{c,k} + \mathbf{z}_t^{c,k}$, where $\alpha_{\mathbf{h}} \in [0, 1]$ is the channel correlation coefficient, $\mathbf{h}_t^{c,k} \sim \mathcal{CN}(\mathbf{0}, \beta^{c,k}\mathbf{I})$ with $\beta^{c,k}$ representing the large-scale fading variation that includes both the path-loss and shadowing, and $\mathbf{z}_t^{c,k} \sim \mathcal{CN}(\mathbf{0}, (1-\alpha_{\mathbf{h}}^2)\beta^{c,k}\mathbf{I})$ is independent of $\mathbf{h}_t^{c,k}$. We set $\beta^{c,k}[\text{dB}] = -31.54 - 33\log_{10}(d^{c,k}) - \psi^{c,k}$ [47], where $d^{c,k}$ is the distance from AP c to user k, and $\psi^{c,k} \sim \mathcal{CN}(0, \sigma_\phi^2)$ models the shadowing effect with $\sigma_\phi^2 = 8$ dB. We set $\alpha_{\mathbf{h}} = 0.998$ as default, which corresponds to the user speed 1 km/h. We emphasize here that the Gauss-Markov channel model is used for illustration only. SOPIP can be applied to any wireless propagation environment, and neither the CC nor the APs needs to know the channel statistics.

[8]Our codes are available at https://github.com/juncheng-wang/SOPIP.

Note that the impact of inaccurate local CSI $\hat{\mathbf{H}}_{t-\tau_l}^c$ can be emulated by increasing the local delay τ_l in $\mathbf{H}_{t-\tau_l}^c$ under the Gauss-Markov channel model. Thus, we assume that each AP c communicates the accurate local CSI $\mathbf{H}_{t-\tau_l}^c$ to the CC at each time t. We assume the CC adopts cooperative ZF precoding as its desired cooperative precoder given by $\mathbf{W}_t^{\text{ZF}} = \sqrt{P_t^{\text{ZF}}} \mathbf{H}_t^H (\mathbf{H}_t \mathbf{H}_t^H)^{-1}$, where P_t^{ZF} is a power normalizing factor. Note that we require $N \geq K$ to perform ZF precoding. The receiver noise power at each user is $\sigma_n^2 = N_F + N_0 B_W$. Thus, by using $\mathbf{W}_t^{\text{ZF}}$, all the users will have the same data rate $\log_2(1 + \frac{P_t^{\text{ZF}}}{\sigma_n^2})$. The CC adopts the following power normalizing factor

$$P_t^{\text{ZF}\star} = \min_{c \in \{1,\ldots,C\}} \frac{P_{\max}^c}{\|\mathbf{H}_t^{cH} (\mathbf{H}_t \mathbf{H}_t^H)^{-1}\|_F^2},$$

which is the optimal solution of the following sum-rate maximization problem with per-AP transmit power limits [49]:

$$\textbf{P2:} \quad \max_{P_t^{\text{ZF}}} \quad K \log_2\left(1 + \frac{P_t^{\text{ZF}}}{\sigma_n^2}\right)$$
$$\text{s.t.} \quad P_t^{\text{ZF}} \|\mathbf{H}_t^{cH} (\mathbf{H}_t \mathbf{H}_t^H)^{-1}\|_F^2 \leq P_{\max}^c, \quad \forall c.$$

To measure the performance, we define the time-averaged normalized precoding deviation as

$$\bar{f}(T) \triangleq \frac{1}{T} \sum_{t=1}^{T} \frac{f_t(\mathbf{V}_t)}{\|\mathbf{H}_t \mathbf{W}_t^{\text{ZF}}\|_F^2}, \quad (44)$$

and the time-averaged per-user rate as

$$\bar{R}(T) \triangleq \frac{1}{TK} \sum_{t=1}^{T} \sum_{k=1}^{K} \log_2(1 + \text{SINR}_t^k) \quad (45)$$

where $\text{SINR}_t^k = \frac{|[\mathbf{H}_t \mathbf{V}_t]_{k,k}|^2}{\sum_{j \neq k} |[\mathbf{H}_t \mathbf{V}_t]_{k,j}|^2 + \sigma_n^2}$ is the signal-to-interference-plus-noise-ratio (SINR) of user k at time slot t.

B. The Impact of The Number of Precoder Update Steps

Fig. 3 and Fig. 4 show $\bar{f}(T)$ and $\bar{R}(T)$ yielded by SOPIP over T, respectively, for different numbers of the precoder update steps J_{CC} at the CC and J_{AP} at the APs. We first consider zero local delay and set the round-trip delay $\tau_r = 1$. We observe that the performance of SOPIP converges fast (within $T = 100$ time slots). Furthermore, the steady-state performance improves as J_{CC} or J_{AP} increases, which demonstrates the performance gain brought by performing multi-step precoder updates with our proposed gradient estimation scheme at both the CC and the APs. As shown in Fig. 3, the steady-state values of $\bar{f}(T)$ and $\bar{R}(T)$ no longer change much when $J_{\text{CC}} \geq 8$. With this and the fact that the APs usually have less computation capacity than the CC, we set $J_{\text{CC}} = 8$ and $J_{\text{AP}} = 4$ as default parameters in the rest of simulation studies presented below.

C. Performance Comparison

For comparison, we consider the following schemes.

- *Delayed Optimal:* The CC collects the global CSI from all APs, computes the optimal cooperative precoder, and sends it to all APs. However, due to communication delay,

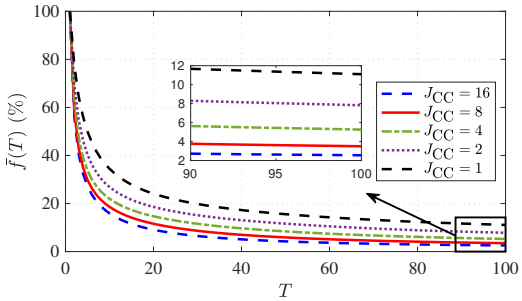

(a) $\bar{f}(T)$ vs. T.

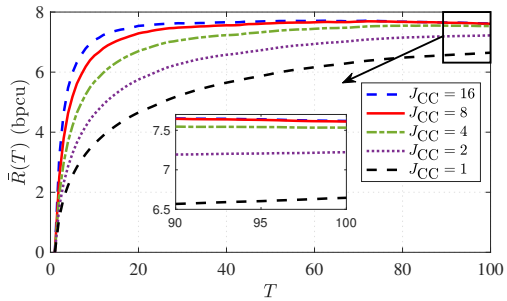

(b) $\bar{R}(T)$ vs. T.

Fig. 3. $\bar{f}(T)$ and $\bar{R}(T)$ vs. T with $J_{\text{AP}} = 1$.

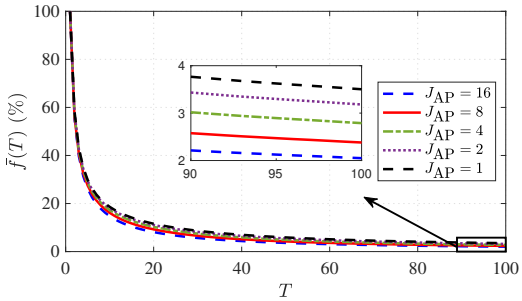

(a) $\bar{f}(T)$ vs. T.

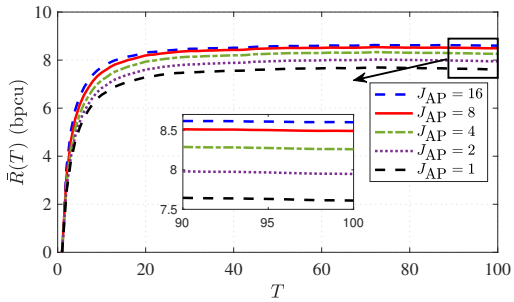

(b) $\bar{R}(T)$ vs. T.

Fig. 4. $\bar{f}(T)$ and $\bar{R}(T)$ vs. T with $J_{\text{CC}} = 8$.

the APs actually execute the delayed precoder $\hat{\mathbf{W}}_{t-\tau}^{\text{ZF}}$ that is received from the CC at each time slot t. Note that the cooperative ZF precoding $\mathbf{W}_t^{\text{ZF}}$ is the optimal solution for the sum-rate maximization problem with per-AP transmit power limits based on the perfect global CSI [49], *i.e.,* **P2**.

- *Centralized OCO:* We run Algorithm 1 at the CC with different numbers of cooperative precoder updates. Each AP c executes the precoder $\hat{\mathbf{V}}_t^{c,J_{\text{CC}}}$ (generated based on the delayed global CSI $\mathbf{H}_{t-\tau}$) that can be received from the CC at each time slot t, without performing any local precoder update. This can be viewed as the centralized OCO approach [42]-[44].[9]
- *Local CSI (LCSI) Dynamic User Association (UA):* We consider the following distributed precoding scheme. Each user k selects the AP with the highest channel gain for downlink transmission at each time slot t based on the local CSI $\mathbf{H}_{t-\tau_l}^c$. Let the number of users associated with AP c be $K_{t-\tau_l}^c$. Let $\bar{\mathbf{H}}_{t-\tau_l}^c \in \mathbb{C}^{K_{t-\tau_l}^c \times N^c}$ denote the available channel state between the $K_{t-\tau_l}^c$ users and AP c. Each AP c adopts ZF precoding to serve the $K_{t-\tau_l}^c$ users at each time slot t, given by $\bar{\mathbf{V}}_t^c = \sqrt{\bar{P}_{t-\tau_l}^c}\bar{\mathbf{H}}_{t-\tau_l}^{cH}(\bar{\mathbf{H}}_{t-\tau_l}^c\bar{\mathbf{H}}_{t-\tau_l}^{cH})^{-1}$, where $\bar{P}_{t-\tau_l}^c$ is set such that $\|\bar{\mathbf{V}}_{t-\tau_l}^c\|_F^2 = P_{\max}^c$.
- *LCSI Fixed UA:* This is a more realistic alternative to *LCSI Dynamic UA*. Each user k selects the AP that has the lowest path loss to the user. The user association does not change during our simulation. The APs operate in the same way as under *LCSI Dynamic UA*.

Fig. 6 and Fig. 5 compare the performance between SOPIP and the alternative schemes in terms of the steady state value of $\bar{f}(T)$ and $\bar{R}(T)$ versus the round-trip delay τ_r and local delay τ_l. Note that $\bar{f}$ is relevant only to SOPIP and *Centralized OCO*. As shown in Fig. 6, for a wide range of τ_r values, SOPIP outperforms the distributed alternatives *LCSI Dynamic UA* and *LCSI Fixed UA*. This demonstrates that even with a large round-trip delay τ_r, performing global precoder updates at the CC using the delayed global information is beneficial for improving the performance. Furthermore, SOPIP outperforms the centralized alternatives *Delayed Optimal* and *Centralized OCO*. This demonstrates the importance of performing local precoder updates at the APs using more timely local CSI. As shorn in Fig. 5, the performance gain of SOPIP over *Centralized OCO* decreases as the local delay τ_l increases. This indicates the importance of timely information on the performance brought by local precoder updates. Overall, we observe that, by fully taking advantage of the timely local CSI at the APs and delayed global CSI at the CC for precoder updates, SOPIP substantially outperforms the other centralized or distributed alternatives over a wide range of delay settings.

In Fig. 7 and Fig. 8, we further study the impacts of the numbers of antennas N^c and users K on the performance of SOPIP with local CSI delay $\tau_l = 0$ and round-trip delay $\tau_r = 4$. Fig. 7 shows that the steady-state per-user rate $\bar{R}$ increases as N^c increases. This is because the APs have more degrees of freedom to design their cooperative precoding. The steady-state per-user rate $\bar{R}$ dramatically improves as N^c increases, showing the precoding gain provided by massive MIMO. Fig. 8 shows that $\bar{R}$ decreases as K increases, due to the increased inter-user interference. Note that for cooperative ZF precoding at the CC, we require $K \leq N = 48$. We observe that SOPIP substantially outperforms *Delayed Optimal* when the K is close to N. Furthermore, in a wide range of N^c and K values, SOPIP yields the best performance among all schemes.

[9] As explained in Section II-D, distributed OCO schemes [29]-[33] are not applicable to **P1**, since they assume separable objective functions.

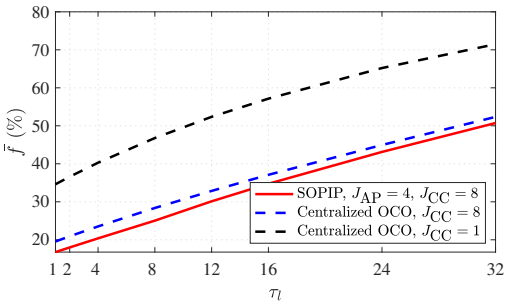

(a) $\bar{f}$ vs. τ_l.

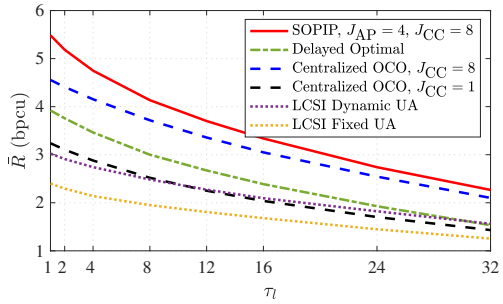

(b) $\bar{R}$ vs. τ_l.

Fig. 5. Performance comparison on $\bar{f}$ and $\bar{R}$ vs. local delay τ_l with round-trip delay $\tau_r = 8$.

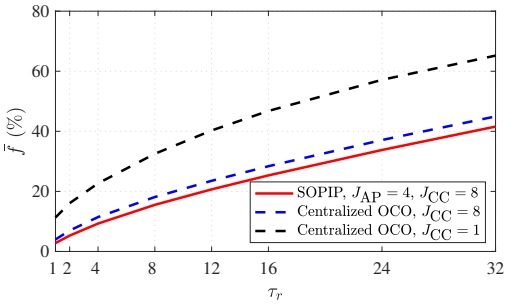

(a) $\bar{f}$ vs. τ_r.

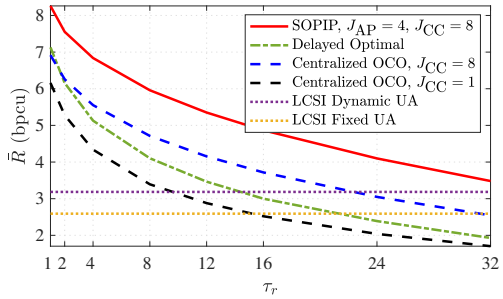

(b) $\bar{R}$ vs. τ_r.

Fig. 6. Performance comparison on $\bar{f}$ and $\bar{R}$ vs. round-trip delay τ_r with local delay $\tau_l = 0$.

VII. Conclusions

We have studied cooperative precoding design in a MIMO network, where multiple APs jointly serve all the users with the assistance of a CC over non-ideal backhaul. We propose an efficient SOPIP algorithm to minimize the accumulated precoding deviation between the actual and desired cooperative precoders, subject to per-AP transmit power limits. SOPIP allows both timely local precoder updates at the APs and delayed cooperative precoder updates at the CC, by effectively parsing the channel and precoder information

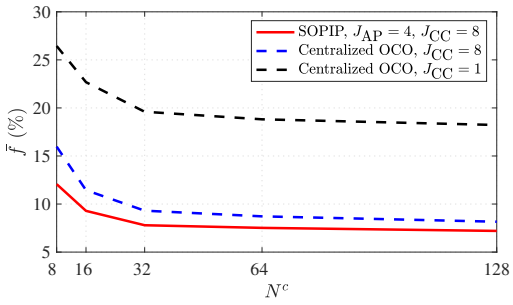

(a) $\bar{f}$ vs. N^c.

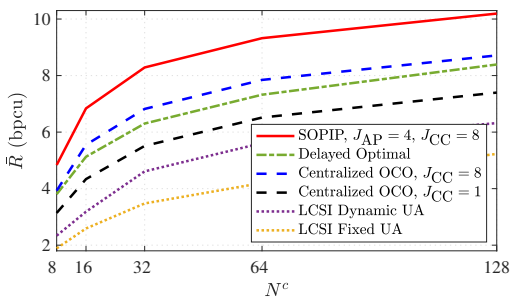

(b) $\bar{R}$ vs. N^c.

Fig. 7. Performance comparison on $\bar{f}$ and $\bar{R}$ vs. N^c with $K = 15$.

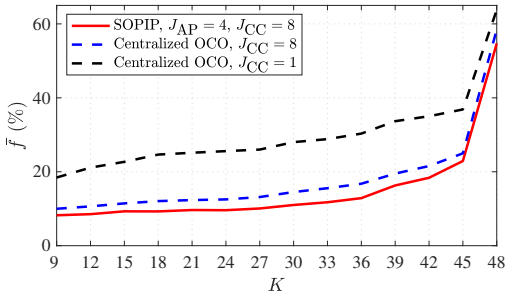

(a) $\bar{f}$ vs. K.

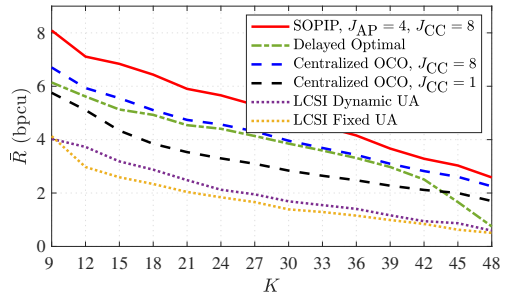

(b) $\bar{R}$ vs. K.

Fig. 8. Performance comparison on $\bar{f}$ and $\bar{R}$ vs. K with $N^c = 16$.

to reduce the communication overhead. Furthermore, SOPIP allows multi-step precoder updates at both the APs and the CC via hierarchical gradient descent to fully utilize their available computational resource. Our performance analysis of SOPIP takes into account of the impacts of the multi-step gradient descent at both the CC and the APs, as well as multi-slot delay, CSI inaccuracy, and gradient estimation error, in deriving the bounds on the performance gap to the optimal solution. Our simulation results demonstrate that SOPIP has the superior tolerance of delay and has a substantial advantage over other centralized and distributed alternatives in a wide rage of scenarios.

Appendix A
Proof of Lemma 1

Proof: Note that $f_t(\mathbf{V}) = \|\mathbf{H}_t\mathbf{V} - \mathbf{H}_t\mathbf{W}_t\|_F^2$ is a squared Frobenius norm. Therefore, $f_t(\mathbf{V})$ is 2-strongly convex w.r.t. $\|\cdot\|_F$.

From $\nabla f_t(\mathbf{V}) = \mathbf{H}_t^H(\mathbf{H}_t\mathbf{V} - \mathbf{H}_t\mathbf{W})$, we have

$$\begin{aligned}
&\|\nabla f_t(\mathbf{U}) - \nabla f_t(\mathbf{V})\|_F \\
&= \|\mathbf{H}_t^H(\mathbf{H}_t\mathbf{U} - \mathbf{H}_t\mathbf{W}) - \mathbf{H}_t^H(\mathbf{H}_t\mathbf{V} - \mathbf{H}_t\mathbf{W})\|_F \\
&= \|\mathbf{H}_t^H\mathbf{H}_t\mathbf{U} - \mathbf{H}_t^H\mathbf{H}_t\mathbf{V}\|_F = \|\mathbf{H}_t^H\mathbf{H}_t(\mathbf{U} - \mathbf{V})\|_F \\
&\overset{(a)}{\leq} \|\mathbf{H}_t\|_F^2\|\mathbf{U} - \mathbf{V}\|_F \overset{(b)}{\leq} B\|\mathbf{U} - \mathbf{V}\|_F
\end{aligned} \tag{46}$$

where (a) follows from $\|\mathbf{AB}\|_F \leq \|\mathbf{A}\|_F\|\mathbf{B}\|_F$ and (b) is because $\|\mathbf{H}_t\|_F^2$ being bounded in (12). The above inequality implies that $\nabla f_t(\mathbf{V})$ is B-Lipschitz continuous. Therefore, $f_t(\mathbf{V})$ is B-smooth.

We now show (15). For any $\mathbf{U}, \mathbf{V} \in \mathcal{V}$, we have

$$\|\mathbf{U} - \mathbf{V}\|_F \overset{(a)}{\leq} \|\mathbf{U}\|_F + \|\mathbf{V}\|_F \overset{(b)}{\leq} 2\sqrt{\sum_{c=1}^{C} P_{\max}^c}. \tag{47}$$

where (a) is because $\|\mathbf{A} + \mathbf{B}\|_F \leq \|\mathbf{A}\|_F + \|\mathbf{B}\|_F$ and (b) follows from $\mathcal{V} = \{\mathbf{V} : \|\mathbf{V}^c\|_F^2 \leq P_{\max}^c, \forall c = 1, \ldots, C\}$ such that $\|\mathbf{V}\|_F^2 = \sum_{c=1}^{C}\|\mathbf{V}^c\|_F^2 \leq \sum_{c=1}^{C} P_{\max}^c$ for any $\mathbf{V} \in \mathcal{V}$.

Finally, we have

$$\begin{aligned}
&\|\nabla f_t(\mathbf{V})\|_F = \|\mathbf{H}_t^H(\mathbf{H}_t\mathbf{V} - \mathbf{H}_t\mathbf{W})\|_F \\
&\leq \|\mathbf{H}_t\|_F\|\mathbf{H}_t\mathbf{V}_t - \mathbf{H}_t\mathbf{W}_t\|_F \\
&\leq \|\mathbf{H}_t\|_F^2\|\mathbf{V}_t - \mathbf{W}_t\|_F \overset{(a)}{\leq} BR
\end{aligned} \tag{48}$$

where (a) follows from the channel power bound in (12) and the precoder feasible set $\mathcal{V}$ being bounded in (15). ■

Appendix B
Proof of Lemma 2

Proof: We first state the property of a μ-strongly convex function below, which is shown in Lemma 2.8 in [28].

Lemma 3. ([28, Lemma 2.8]) Let $\mathcal{X} \in \mathbb{R}^n$ be a nonempty convex set. Let $h(\mathbf{x}) : \mathbb{R}^n \to \mathbb{R}$ be a μ-strongly convex function over $\mathcal{X}$ with respect to a norm $\|\cdot\|$. Let $\mathbf{y} = \arg\min_{\mathbf{x}\in\mathcal{X}}\{h(\mathbf{x})\}$. Then, for any $\mathbf{z} \in \mathcal{X}$, we have $h(\mathbf{y}) \leq h(\mathbf{z}) - \frac{\mu}{2}\|\mathbf{z} - \mathbf{y}\|^2$.

Note that $\mathbf{U}$ is the optimal solution to the following optimization problem

$$\min_{\mathbf{W}\in\mathcal{V}} \quad \langle\nabla\hat{f}_t(\mathbf{V}), \mathbf{W} - \mathbf{V}\rangle_F + \frac{\alpha}{2}\|\mathbf{W} - \mathbf{V}\|_F^2.$$

Since the objective of the above optimization problem is α-strongly convex w.r.t. $\|\cdot\|_F$, from Lemma 3, we have

$$\begin{aligned}
&\langle\nabla f_t(\mathbf{V}), \mathbf{U} - \mathbf{V}\rangle_F + \frac{\alpha}{2}\|\mathbf{U} - \mathbf{V}\|_F^2 \\
&\quad + \langle\nabla\hat{f}_t(\mathbf{V}) - \nabla f_t(\mathbf{V}), \mathbf{U} - \mathbf{V}\rangle_F \\
&\leq \langle\nabla f_t(\mathbf{V}), \mathbf{W}_t - \mathbf{V}\rangle_F + \frac{\alpha}{2}\|\mathbf{W}_t - \mathbf{V}\|_F^2 - \frac{\alpha}{2}\|\mathbf{U} - \mathbf{W}_t\|_F^2 \\
&\quad + \langle\nabla\hat{f}_t(\mathbf{V}) - \nabla f_t(\mathbf{V}), \mathbf{W}_t - \mathbf{V}\rangle_F.
\end{aligned} \tag{49}$$

From $f_t(\mathbf{x})$ being 2-strongly convex in (13), we have

$$f_t(\mathbf{W}_t) \geq f_t(\mathbf{V}) + \langle\nabla f_t(\mathbf{V}), \mathbf{W}_t - \mathbf{V}\rangle_F + \|\mathbf{W}_t - \mathbf{V}\|_F^2. \tag{50}$$

Adding $f_t(\mathbf{V})$ on both sides of (49), applying (14) and (50) respectively to the left-hand side (LHS) and right-hand side (RHS) of (49), we have

$$\begin{aligned}
&f_t(\mathbf{U}) - \frac{B}{2}\|\mathbf{U} - \mathbf{V}\|_F + \frac{\alpha}{2}\|\mathbf{U} - \mathbf{V}\|_F^2 \\
&\quad + \langle\nabla\hat{f}_t(\mathbf{V}) - \nabla f_t(\mathbf{V}), \mathbf{U} - \mathbf{V}\rangle_F \\
&\leq f_t(\mathbf{W}_t) - \|\mathbf{W}_t - \mathbf{V}\|_F^2 + \frac{\alpha}{2}\|\mathbf{W}_t - \mathbf{V}\|_F^2 - \frac{\alpha}{2}\|\mathbf{U} - \mathbf{W}_t\|_F^2 \\
&\quad + \langle\nabla\hat{f}_t(\mathbf{V}) - \nabla f_t(\mathbf{V}), \mathbf{W}_t - \mathbf{V}\rangle_F.
\end{aligned} \tag{51}$$

Rearranging terms of (51), we have

$$\begin{aligned}
&f_t(\mathbf{U}) - \frac{B}{2}\|\mathbf{U} - \mathbf{V}\|_F^2 + \frac{\alpha}{2}\|\mathbf{U} - \mathbf{V}\|_F^2 \\
&\leq f_t(\mathbf{W}_t) + \frac{\alpha - 2}{2}\|\mathbf{W}_t - \mathbf{V}\|_F^2 - \frac{\alpha}{2}\|\mathbf{U} - \mathbf{W}_t\|_F^2 \\
&\quad + \langle\nabla f_t(\mathbf{V}) - \nabla\hat{f}_t(\mathbf{V}), \mathbf{U} - \mathbf{W}_t\rangle_F.
\end{aligned} \tag{52}$$

Since $\mathbf{W}_t \in \arg\min_{\mathbf{V}\in\mathcal{V}} f_t(\mathbf{V})$ and $f_t(\mathbf{V})$ is 2-strongly convex as in (13), from Lemma 3, we have

$$f_t(\mathbf{W}_t) \leq f_t(\mathbf{U}) - \|\mathbf{U} - \mathbf{W}_t\|_F^2. \tag{53}$$

Applying (53) to the RHS of (52) and rearranging terms, we have

$$\begin{aligned}
&\frac{\alpha + 2}{2}\|\mathbf{U} - \mathbf{W}_t\|_F^2 + \frac{\alpha - B}{2}\|\mathbf{U} - \mathbf{V}\|_F^2 \\
&\leq \frac{\alpha - 2}{2}\|\mathbf{V} - \mathbf{W}_t\|_F^2 + \langle\nabla f_t(\mathbf{V}) - \nabla\hat{f}_t(\mathbf{V}), \mathbf{U} - \mathbf{W}_t\rangle_F \\
&\overset{(a)}{\leq} \frac{\alpha - 2}{2}\|\mathbf{V} - \mathbf{W}_t\|_F^2 + \frac{\gamma}{2}\|\mathbf{U} - \mathbf{W}_t\|_F^2 \\
&\quad + \frac{2}{\gamma}\|\nabla f_t(\mathbf{V}) - \hat{\nabla} f_t(\mathbf{V})\|_F^2
\end{aligned} \tag{54}$$

where (a) follows from $\langle\mathbf{A}, \mathbf{B}\rangle_F = 2\Re\{\mathrm{tr}\{\mathbf{A}^H\mathbf{B}\}\} \leq \frac{2}{\gamma}\|\mathbf{A}\|_F^2 + \frac{\gamma}{2}\|\mathbf{B}\|_F^2, \forall\gamma > 0$.

Rearranging terms on both sides of (54), we have

$$\begin{aligned}
&\frac{\alpha + 2 - \gamma}{2}\|\mathbf{U} - \mathbf{W}_t\|_F^2 + \frac{\alpha - B}{2}\|\mathbf{U} - \mathbf{V}\|_F^2 \\
&\leq \frac{\alpha - 2}{2}\|\mathbf{V} - \mathbf{W}_t\|_F^2 + \frac{2}{\gamma}\|\nabla f_t(\mathbf{V}) - \hat{\nabla} f_t(\mathbf{V})\|_F^2.
\end{aligned} \tag{55}$$

Note that $B \geq 2$. Therefore, if $\alpha \geq B$ and $\gamma < 4$, we have $\alpha + 2 - \gamma > 0$. Multiplying both sides of (55) by $\frac{2}{\alpha+2-\gamma}$, we have (17). ■

References

[1] J. Wang, B. Liang, M. Dong, G. Boudreau, and H. Abou-Zeid, "Semi-online precoding with information parsing for cooperative MIMO wireless networks," in *Proc. IEEE Conf. Comput. Commun. (INFOCOM)*, 2022.

[2] V. Jungnickel, K. Manolakis, W. Zirwas, B. Panzner, V. Braun, M. Lossow, M. Sternad, R. Apelfrjd, and T. Svensson, "The role of small cells, coordinated multipoint, and massive MIMO in 5G," *IEEE Commun. Mag.*, vol. 52, pp. 44–51, May 2014.

[3] T. L. Marzetta, "Noncooperative cellular wireless with unlimited numbers of base station antennas," *IEEE Trans. Wireless Commun.*, vol. 9, pp. 3590–3600, Nov. 2010.

[4] D. Gesbert, S. Hanly, H. Huang, S. Shamai Shitz, O. Simeone, and W. Yu, "Multi-cell MIMO cooperative networks: A new look at interference," *IEEE J. Sel. Areas Commun.*, vol. 28, pp. 1380–1408, Dec. 2010.

[5] D. Lee, H. Seo, B. Clerckx, E. Hardouin, D. Mazzarese, S. Nagata, and K. Sayana, "Coordinated multipoint transmission and reception in LTE-advanced: deployment scenarios and operational challenges," *IEEE Commun. Mag.*, vol. 50, pp. 148–155, Feb. 2012.

[6] J. Wu, Z. Zhang, Y. Hong, and Y. Wen, "Cloud radio access network (C-RAN): a primer," *IEEE Netw.*, vol. 29, pp. 35–41, Jan. 2015.

[7] J. Zhang, S. Chen, Y. Lin, J. Zheng, B. Ai, and L. Hanzo, "Cell-free massive MIMO: A new next-generation paradigm," *IEEE Access*, vol. 7, pp. 99 878–99 888, Jul. 2019.

[8] O. Somekh, O. Simeone, Y. Bar-Ness, A. M. Haimovich, and S. Shamai, "Cooperative multicell zero-forcing beamforming in cellular downlink channels," *IEEE Trans. Inf. Theory*, vol. 55, pp. 3206–3219, Jul. 2009.

[9] H. Zhang, N. B. Mehta, A. F. Molisch, J. Zhang, and S. H. Dai, "Asynchronous interference mitigation in cooperative base station systems," *IEEE Trans. Wireless Commun.*, vol. 7, no. 1, pp. 155–165, Jan. 2008.

[10] R. Zhang, "Cooperative multi-cell block diagonalization with per-base-station power constraints," *IEEE J. Sel. Areas Commun.*, vol. 28, pp. 1435–1445, Dec. 2010.

[11] S.-H. Park, O. Simeone, O. Sahin, and S. Shamai, "Joint precoding and multivariate backhaul compression for the downlink of cloud radio access networks," *IEEE Trans. Signal Process.*, vol. 61, pp. 5646–5658, Nov. 2013.

[12] B. Dai and W. Yu, "Energy efficiency of downlink transmission strategies for cloud radio access networks," *IEEE J. Sel. Areas Commun.*, vol. 34, pp. 1037–1050, Apr. 2016.

[13] F. Zhuang and V. K. N. Lau, "Backhaul limited asymmetric cooperation for MIMO cellular networks via semidefinite relaxation," *IEEE Trans. Signal Process.*, vol. 62, no. 3, pp. 684–693, Feb. 2014.

[14] H. Q. Ngo, A. Ashikhmin, H. Yang, E. G. Larsson, and T. L. Marzetta, "Cell-free massive MIMO versus small cells," *IEEE Trans. Wireless Commun.*, vol. 16, pp. 1834–1850, Mar. 2017.

[15] E. Nayebi, A. Ashikhmin, T. L. Marzetta, H. Yang, and B. D. Rao, "Precoding and power optimization in cell-free massive MIMO systems," *IEEE Trans. Wireless Commun.*, vol. 16, pp. 4445–4459, Jul. 2017.

[16] R. Zakhour and D. Gesbert, "Distributed multicell-MISO precoding using the layered virtual SINR framework," *IEEE Trans. Wireless Commun.*, vol. 9, pp. 2444–2448, Aug. 2010.

[17] E. Bjrnson, R. Zakhour, D. Gesbert, and B. Ottersten, "Cooperative multicell precoding: Rate region characterization and distributed strategies with instantaneous and statistical CSI," *IEEE Trans. Signal Process.*, vol. 58, pp. 4298–4310, Aug. 2010.

[18] J. Zhang, X. Yuan, and L. Ping, "Hermitian precoding for distributed MIMO systems with individual channel state information," *IEEE J. Sel. Areas Commun.*, vol. 31, pp. 241–250, Feb. 2013.

[19] M. Hong, R. Sun, H. Baligh, and Z.-Q. Luo, "Joint base station clustering and beamformer design for partial coordinated transmission in heterogeneous networks," *IEEE J. Sel. Areas Commun.*, vol. 31, pp. 226–240, 2013.

[20] J. Kaleva, A. Tlli, M. Juntti, R. A. Berry, and M. L. Honig, "Decentralized joint precoding with pilot-aided beamformer estimation," *IEEE Trans. Signal Process.*, vol. 66, pp. 2330–2341, May 2018.

[21] R. Yao, Y. Liu, L. Lu, G. Y. Li, and A. Maaref, "Cooperative precoding for cognitive transmission in two-tier networks," *IEEE Trans. Commun.*, vol. 64, no. 4, pp. 1423–1436, Apr. 2016.

[22] F. Wang, L. Ruan, and M. Z. Win, "Cooperative network operation design for mobility-aware cloud radio access network," *IEEE Trans. Wireless Commun.*, vol. 17, no. 12, pp. 7819–7833, Dec. 2018.

[23] E. Bjrnson and L. Sanguinetti, "Making cell-free massive MIMO competitive with MMSE processing and centralized implementation," *IEEE Trans. Wireless Commun.*, vol. 19, pp. 77–90, Jan. 2020.

[24] P. Mertikopoulos and A. L. Moustakas, "Learning in an uncertain world: MIMO covariance matrix optimization with imperfect feedback," *IEEE Trans. Signal Process.*, vol. 64, pp. 5–18, Jan. 2016.

[25] H. Yu and M. J. Neely, "Dynamic transmit covariance design in MIMO fading systems with unknown channel distributions and inaccurate channel state information," *IEEE Trans. Wireless Commun.*, vol. 16, pp. 3996–4008, Jun. 2017.

[26] J. Wang, M. Dong, B. Liang, and G. Boudreau, "Periodic updates for constrained OCO with application to large-scale multi-antenna systems," *IEEE Trans. Mobile Comput.*, Aug. 2022, early access.

[27] Y. Dong, H. Zhang, J. Li, F. R. Yu, S. Guo, and V. C. M. Leung, "An online zero-forcing precoder for weighted sum-rate maximization in green CoMP systems," *IEEE Trans. Wireless Commun.*, vol. 21, pp. 7566–7581, Sep. 2022.

[28] S. Shalev-Shwartz, "Online learning and online convex optimization," *Found. Trends Mach. Learn.*, vol. 4, pp. 107–194, Feb. 2012.

[29] S. Hosseini, A. Chapman, and M. Mesbahi, "Online distributed optimization via dual averaging," in *Proc. IEEE Conf. Decision Control (CDC)*, 2013.

[30] D. Mateos-Nunez and J. Cortes, "Distributed online convex optimization over jointly connected digraphs," *IEEE Trans. Netw. Sci. Eng.*, vol. 1, pp. 23–37, Oct. 2014.

[31] S. Shahrampour and A. Jadbabaie, "Distributed online optimization in dynamic environments using mirror descent," *IEEE Trans. Automat. Contr.*, vol. 63, pp. 714–725, Mar. 2018.

[32] Y. Zhang, R. J. Ravier, M. M. Zavlanos, and V. Tarokh, "A distributed online convex optimization algorithm with improved dynamic regret," in *Proc. IEEE Conf. Decision Control (CDC)*, 2019.

[33] N. Eshraghi and B. Liang, "Distributed online optimization over a heterogeneous network with any-batch mirror descent," in *Proc. Intel. Conf. Mach. Learn. (ICML)*, 2020.

[34] H. Dahrouj and W. Yu, "Coordinated beamforming for the multicell multi-antenna wireless system," *IEEE Trans. Wireless Commun.*, vol. 9, pp. 1748–1759, May 2010.

[35] L. Venturino, N. Prasad, and X. Wang, "Coordinated linear beamforming in downlink multi-cell wireless networks," *IEEE Trans. Wireless Commun.*, vol. 9, pp. 1451–1461, Apr. 2010.

[36] I. Boukhedimi, A. Kammoun, and M.-S. Alouini, "Coordinated SLNR based precoding in large-scale heterogeneous networks," *IEEE J. Sel. Topics Signal Process.*, vol. 11, pp. 534–548, Apr. 2017.

[37] J. Bai, T. Dong, Q. Zhang, S. Wang, and N. Li, "Coordinated beamforming and artificial noise in the downlink secure multi-cell MIMO systems under imperfect CSI," *IEEE Wireless Commun. Lett.*, vol. 9, pp. 1023–1026, Jul. 2020.

[38] D. Wu and H. Zhang, "Tractable modelling and robust coordinated beamforming design with partially accurate CSI," *IEEE Wireless Commun. Lett.*, vol. 10, pp. 2384–2387, Nov. 2021.

[39] M. Zinkevich, "Online convex programming and generalized infinitesimal gradient ascent," in *Proc. Intel. Conf. Mach. Learn. (ICML)*, 2003.

[40] E. Hazan, A. Agarwal, and S. Kale, "Logarithmic regret algorithms for online convex optimization," *Mach. Learn.*, vol. 69, pp. 169–192, 2007.

[41] A. Jadbabaie, A. Rakhlin, S. Shahrampour, and K. Sridharan, "Online optimization: Competing with dynamic comparators," in *Proc. Intel. Conf. Artif. Intell. Statist. (AISTATS)*, 2015.

[42] A. Mokhtari, S. Shahrampour, A. Jababaie, and A. Ribeiro, "Online optimization in dynamic environments: Improved regret rates for strongly convex problems," in *Proc. IEEE Conf. Decision Control (CDC)*, 2016.

[43] L. Zhang, T. Yang, J. Yi, J. Rong, and Z.-H. Zhou, "Improved dynamic regret for non-degenerate functions," in *Proc. Adv. Neural Info. Proc. Sys. (NIPS)*, 2017.

[44] A. S. Bedi, P. Sarma, and K. Rajawat, "Tracking moving agents via inexact online gradient descent algorithm," *IEEE J. Sel. Topics Signal Process.*, vol. 12, pp. 202–217, 2018.

[45] J. Wang, B. Liang, M. Dong, G. Boudreau, and H. Abou-Zeid, "Delay-tolerant constrained OCO with application to network resource allocation," in *IEEE Conf. Comput. Commun. (INFOCOM)*, 2021.

[46] J. Wang, M. Dong, B. Liang, G. Boudreau, and H. Abou-Zeid, "Delay-tolerant OCO with long-term constraints: Algorithm and its application to network resource allocation," *IEEE/ACM Trans. Netw.*, Jul. 2022, early access.

[47] H. Holma and A. Toskala, *WCDMA for UMTS - HSPA evolution and LTE*. John Wiely & Sons, 2010.

[48] I. Abou-Faycal, M. Medard, and U. Madhow, "Binary adaptive coded pilot symbol assisted modulation over rayleigh fading channels without feedback," *IEEE Trans. Commun.*, vol. 53, pp. 1036–1046, Jun. 2005.

[49] K. Karakayali, R. Yates, G. Foschini, and R. Valenzuela, "Optimum zero-forcing beamforming with per-antenna power constraints," in *Proc. IEEE Symposium on Inform. Theory (ISIT)*, 2007.

Juncheng Wang (Member, IEEE) received the B.Eng. degree in Electrical Engineering from Shanghai Jiao Tong University, Shanghai, China, in 2014, the M.Sc. degree in Electrical and Computer Engineering from the University of Alberta, Edmonton, AB, Canada, in 2017, and the Ph.D. degree in Electrical and Computer Engineering from the University of Toronto, Toronto, ON, Canada, in 2023. He is currently an Assistant Professor with the Department of Computer Science, Hong Kong Baptist University, Hong Kong, China. His research interests include communication networks, online learning, distributed computing, and stochastic optimization.

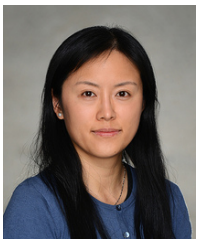

Min Dong (Senior Member, IEEE) received the B.Eng. degree from Tsinghua University, Beijing, China, in 1998, and the Ph.D. degree in electrical and computer engineering with a minor in applied mathematics from Cornell University, Ithaca, NY, in 2004. From 2004 to 2008, she was with Qualcomm Research, Qualcomm Inc., San Diego, CA. Since 2008, she has been with Ontario Tech University, where she is currently a Professor in the Department of Electrical, Computer and Software Engineering. She also holds a status-only Professor appointment with the Department of Electrical and Computer Engineering at the University of Toronto. Her research interests include wireless communications, statistical signal processing, learning techniques, optimization and control applications in cyber-physical systems.

Dr. Dong received the Early Researcher Award from the Ontario Ministry of Research and Innovation in 2012, the Best Paper Award at IEEE ICCC in 2012, and the 2004 IEEE Signal Processing Society Best Paper Award. She is a co-author of the Best Student Paper at IEEE SPAWC 2021 and the Best Student Paper of Signal Processing for Communications and Networking at IEEE ICASSP 2016. She is an Editor for the IEEE TRANSACTIONS ON WIRELESS COMMUNICATIONS and IEEE OPEN JOURNAL of SIGNAL PROCESSING. She was an Associate Editor for the IEEE TRANSACTIONS ON SIGNAL PROCESSING (2010-2014) and the IEEE SIGNAL PROCESSING LETTERS (2009-2013). She was also on the Steering Committee of the IEEE TRANSACTIONS ON MOBILE COMPUTING (2019-2021). She was an elected member of the Signal Processing for Communications and Networking (SP-COM) Technical Committee of IEEE Signal Processing Society (2013-2018). She was the lead Co-Chair of the Communications and Networks to Enable the Smart Grid Symposium at the IEEE International Conference on Smart Grid Communications in 2014.

Ben Liang (Fellow, IEEE) received honors-simultaneous B.Sc. (valedictorian) and M.Sc. degrees in Electrical Engineering from Polytechnic University (now the engineering school of New York University) in 1997 and the Ph.D. degree in Electrical Engineering with a minor in Computer Science from Cornell University in 2001. He was a visiting lecturer and postdoctoral research associate at Cornell University in the 2001 - 2002 academic year. He joined the Department of Electrical and Computer Engineering at the University of Toronto in 2002, where he is now Professor and L. Lau Chair in Electrical and Computer Engineering. His current research interests are in networked systems and mobile communications. He is an associate editor for the IEEE Transactions on Mobile Computing and has served on the editorial boards of the IEEE Transactions on Communications, the IEEE Transactions on Wireless Communications, and the Wiley Security and Communication Networks. He regularly serves on the organizational and technical committees of a number of conferences. He is a Fellow of IEEE and a member of ACM and Tau Beta Pi.

Gary Boudreau (Senior Member, IEEE) received a B.A.Sc. in Electrical Engineering from the University of Ottawa in 1983, an M.A.Sc. in Electrical Engineering from Queens University in 1984 and a Ph.D. in electrical engineering from Carleton University in 1989. From 1984 to 1989 he was employed as a communications systems engineer with Canadian Astronautics Limited and from 1990 to 1993 he worked as a satellite systems engineer for MPR Teltech Ltd. For the period spanning 1993 to 2009 he was employed by Nortel Networks in a variety of wireless systems and management roles within the CDMA and LTE basestation product groups. In 2010 he joined Ericsson Canada where he is currently Director of RAN Architecture and Performance in the North American CTO office. His interests include digital and wireless communications, signal processing and machine learning.

Hatem Abou-Zeid (Member, IEEE) received the Ph.D. degree in electrical and computer engineering from Queens University in 2014. From 2015 to 2017, he was at Cisco Systems designing scalable traffic engineering and routing solutions for service provider networks. Prior to joining the University of Calgary, he was at Ericsson Canada for 4 years leading 5G radio access designs and contributing to intellectual property development in the areas of RAN intelligence, low latency communications, spectrum sharing, and interference mitigation. Several wireless access algorithms and traffic engineering techniques that he co-invented and co-developed are deployed in 5G mobile networks worldwide. He is also an Adjunct Professor at Queens University, Ontario Tech University, and Carleton University in Canada.

Dr. Abou-Zeid's research interests are broadly in 6G wireless networking, robust artificial intelligence, and extended reality communications. His work has resulted in 19 patent filings and 60 journal and conference publications in several IEEE flagship venues, and he is a co-author of a Best Paper Award at IEEE ICC 2022. He is an avid supporter of industry-university partnerships, and he served on the Ericsson Government Industry Relations and Talent Development Committees where he directed multiple academic research partnerships. He also served on the TPC of several IEEE Conferences and was the Co-Chair of the IEEE ICC Workshop on Wireless Network Innovations for Mobile Edge Learning, and Corporate Co-Chair of the IEEE LCN Conference 2022. He received the Software Engineering Professor of the Year and Early Research Excellence Awards in 2023 at University of Calgary, was awarded a DAAD RISE Fellowship at Bell Labs, and nominated for an Outstanding Thesis Medal at Queens University.